GFZ
Helmholtz-Zentrum
POTSDAM

Originally published as:

Fuchs, S., Förster, A. (2014): Well-log based prediction of thermal conductivity of sedimentary successions: a case study from the North German Basin. - *Geophysical Journal International*, *196*, 1, 291-311

DOI: 10.1093/gji/ggt382

Geophysical Journal International

Geophys. J. Int. (2013) doi: 10.1093/gji/ggt382

Geophysical Journal International Advance Access published November 19, 2013

Well-log based prediction of thermal conductivity of sedimentary successions: a case study from the North German Basin

Sven Fuchs[1] and Andrea Förster[2]

[1]*Department of Geosciences, Aarhus University, Høegh-Guldbergs Gade 2, DK-8000 Aarhus C, Denmark. E-mail: fuchs@geo.au.dk*
[2]*Section 4.1 Reservoir Technologies, GFZ German Research Centre for Geosciences, Telegrafenberg, D-14473 Potsdam, Germany*

Accepted 2013 September 17. Received 2013 September 11; in original form 2013 April 16

SUMMARY

Data on rock thermal conductivity (TC) are important for the quantification of the subsurface temperature regime and for the determination of heat flow. If drill core is not retrieved from boreholes and thus no laboratory measurement of TC can be made, other methods are desired to determine TC. One of these methods is the prediction of TC from well logs. We have examined the relationships between TC and standard well-log data (gamma ray, density, sonic interval transit time, hydrogen index and photoelectric factor) by a theoretical analysis and by using real subsurface data from four boreholes of the North German Basin. The theoretical approach comprised the calculation of TC from well-log response values for artificial sets of mineral assemblages consisting of variable contents of 15 rock-forming minerals typical for sedimentary rocks. The analysis shows different correlation trends between TC and the theoretical well-log response in dependence on the mineral content, affecting the rock matrix TC, and on porosity. The analysis suggests the development of empirical equations for the prediction of matrix TC separately for different groups of sedimentary rocks. The most valuable input parameters are the volume fraction of shale, the matrix hydrogen index and the matrix density. The error of matrix TC prediction is on the order of 4.2 ± 3.2 per cent (carbonates), 7.0 ± 5.6 per cent (evaporites), and 11.4 ± 9.1 per cent (clastic rocks). From the subsurface data, comprising measured TC values ($n = 1755$) and well-log data, four prediction equations for bulk TC were developed resembling different lithological compositions. The most valuable input parameters for these predictions are the volume fraction of shale, the hydrogen index and the sonic interval transit time. The equations predict TC with an average error between 5.5 ± 4.1 per cent (clean sandstones of low porosity; Middle Buntsandstein), 8.9 ± 5.4 per cent (interbedding of sandstone, silt- and claystones; Wealden), and 9.4 ± 11 per cent (shaly sandstones; Stuttgart Fm.). An equation including all clastic rock data yields an average error of 11 ± 10 per cent. The subsurface data set also was used to validate the prediction equation for matrix TC established for clastic rocks. Comparison of bulk TC, computed from the matrix TC values and well-log porosity according to the geometric-mean model, to measured bulk TC results in an accuracy <15 per cent. A validation of the TC prediction at borehole scale by comparison of measured temperature logs and modeled temperature logs (based on the site-specific surface heat flow and the predicted TC) shows an excellent agreement in temperature. Interval temperature gradients vary on average by <3 K km^{-1} and predicted compared to measured absolute temperature fitted with an accuracy <5 per cent. Compared to previously published TC prediction approaches, the developed matrix and bulk TC prediction equations show significantly higher prediction accuracy. Bulk TC ranging from 1.5 to 5.5 W (m K)$^{-1}$ is always predicted with an average error <10 per cent relative to average errors between 15 and 35 per cent resulting from the application to our data set of the most suitable methods from literature.

Key words: Downhole methods; Heat flow; Sedimentary basin processes; Heat generation and transport; Europe.

GJI Mineral physics, rheology, heat flow and volcanology

Downloaded from http://gji.oxfordjournals.org/ at Bibliothek des Wissenschaftsparks Albert Einstein on November 20, 2013

© The Authors 2013. Published by Oxford University Press on behalf of The Royal Astronomical Society.

1 INTRODUCTION

Thermal conductivity (TC, λ) is an intrinsic physical property of minerals and rocks. In sedimentary basins, where the sedimentary record usually is very heterogeneous exposing various lithotypes of different mineralogy, rock TC can vary both laterally and vertically thus altering the basin's thermal structure locally and regionally. Knowledge of the TC of geological formations and its spatial variations is fundamental for quantifying the basin evolution, hydrocarbon maturation processes, but also for understanding the geothermal condition of a geological setting. Furthermore, the TC forms in conjunction with the temperature gradient (*gradT*), according to Fourier's law, the basic input parameter for the heat-flow density (q) determination of an area, which in turn is a major input parameter in temperature modeling at different scale, also including deeper crustal levels.

Subsurface rock TC usually is determined by laboratory measurements on drill cuttings or core samples recovered from boreholes. Different techniques are available for these measurements, comprising steady-state and transient techniques (e.g. von Herzen & Maxwell 1959; Beck 1965; Sass *et al.* 1971; Vacquier 1985; Popov *et al.* 1999).

However, as rock samples are often restricted only to some target reservoir, the TC for entire borehole profiles usually cannot be determined. Therefore, methodologies are desired to quantify the TC indirectly from a suite of other petrophysical properties measured by well logs. Such an approach would allow the determination of TC in a profile-wise fashion and, in the best situation, along an entire borehole section. Various data sets and regression parameters are known from several studies performed in different geological environments, but, up to date, no universal well-log based prediction equation for TC is developed yet. Such a universally valid prediction would need to be calculated from a global, comprehensive data set of TC measured for a full spectrum of sedimentary rocks (Williams & Anderson 1990) and, in turn, from a well-log data set that can fully reflect and explain the TC variability within the 'global data set'.

In this paper, we address the indirect determination of TC from petrophysical well-log properties obtained in sedimentary rocks. The study specifically aims to answer the following critical questions: (1) what well-log data/parameters are most valuable in predicting TC; (2) can any universally valid statistical prediction equation be developed using conventional well logs, and if not, how can this problem circumnavigated; (3) what are major limiting factors in the well-log based approach and (4) what method shows the highest prediction quality?

2 BACKGROUND ON TC PREDICTION FROM WELL LOGS

Several approaches exist to determine TC in boreholes. High-precision equilibrium temperature logs can be inverted for an indirect determination of TC by applying a value of heat-flow density to the entire log after having calculated an interval heat-flow density from TC measured on drill core and from an average temperature gradient of this particular depth interval (e.g. Blackwell & Steele 1989; Fuchs & Förster 2010). However, the major drawback is that measurements of equilibrium temperature logs are rarely available. Up to now, this approach is still academic and not standard in the exploration of resources.

The utilization of petrophysical well logs to determine TC is another basic approach. One type of methods hereby applies an appropriate mixing law to compute rock TC from the TC of mineral constituents (e.g. provided by XRD analysis) and well-log-derived rock porosity (e.g. Brigaud *et al.* 1990; Demongodin *et al.* 1991). Other methods derive either the lithology or the major mineralogy of a borehole section from well logs using an inverse solution and typical log-response values of each component (Savre 1963; Doveton & Cable 1979; Quirein *et al.* 1986), and, in turn, apply an appropriate mixing equation to calculate bulk TC for the respective lithotype using textbook TC values (e.g. Merkel *et al.* 1976; Dove & Williams 1989; Brigaud *et al.* 1990; Demongodin, *et al.* 1991; Vasseur *et al.* 1995; Midttømme *et al.* 1997; Hartmann *et al.* 2005). Major uncertainties with this method are linked with the well-log quality, the local complexity of rock composition, and the log-reference values selected. Another method applies the phonon-conduction theory to predict TC for crystalline rocks using density, sonic velocity, and temperature as predictor variables (Williams & Anderson 1990). However, the temperature data required in this approach hinder an application in wells, in which only standard well logs are measured.

Numerous authors have demonstrated for different rock types the direct relation of TC and single petrophysical properties (mostly density and sonic velocity) using statistical methods (e.g. Čermák 1967; Anand *et al.* 1973; Poulsen *et al.* 1981; Beziat *et al.* 1992; Pribnow *et al.* 1993; Kukkonen & Peltoniemi 1998; Sundberg 2002; Popov *et al.* 2003; Hartmann *et al.* 2005, 2008; Goutorbe *et al.* 2006; Sundberg *et al.* 2009; Gegenhuber & Schön 2012). However, the results gained for sedimentary as well as crystalline rocks show inconsistencies, are inhomogeneous, and the observed correlation trends differ significantly from one another. Some data show just scatter, some a positive correlation and other a negative correlation of bulk TC with different properties. Hence, no generally valid, simple linear correlation between TC and density or sonic velocity seems to exist, which is in accordance to conclusions by Kukkonen & Peltoniemi (1998). The list of empirical relationships established between well-log data and measured TC is long. Also the complexity of the proposed equations is quite different due to the developed calculation models (e.g. Houbolt & Wells 1980; Gegenhuber & Schön 2012) or because of different regression techniques applied. Simple linear regression (SLR; Dachnov & Djakonov 1952; Zierfuss & Van der Vliet 1956; Bullard & Day 1961; Karl 1965; Moiseyenko *et al.* 1970; Molnar & Hodge 1982; Lovell & Ogden 1984; Lovell 1985; Della Vedova & Von Herzen 1987; Griffiths *et al.* 1992; Zamora *et al.* 1993; Sahlin & Middleton 1997; Popov *et al.* 2011), multiple linear regression (MLR; e.g. Thornton 1924; Anand *et al.* 1973; Goss *et al.* 1975; Goss & Combs 1976; Evans 1977; Molnar & Hodge 1982; Vacquier *et al.* 1988; Doveton *et al.* 1997; Popov *et al.* 2003; Hartmann *et al.* 2005; Goutorbe *et al.* 2006; Khandelwal 2010) as well as non-linear regression (NLR) analysis (e.g. Tikhomirov 1968; Balling *et al.* 1981; Özkahraman *et al.* 2004; Popov *et al.* 2011) were used. These regression-based empirical equations are typically limited to the rocks on the basis of which they were established (e.g. lithotype, stratigraphy) so that they are not universally applicable (e.g. Goss & Combs 1976; Evans 1977; Molnar & Hodge 1982; Blackwell & Steele 1989; Hartmann *et al.* 2005). Most recently, studies were published that use artificial neuronal networks (ANNs) instead of linear or even NLR techniques (e.g. Goutorbe *et al.* 2006; Singh *et al.* 2007; Singh *et al.* 2011; Khandelwal 2010). The ANNs often show higher accuracy compared to common regression techniques. However, due the lack of knowledge on the internal parameters deployed they do not allow a third party to use them later on for their own TC prediction.

Downloaded from http://gji.oxfordjournals.org/ at Bibliothek des Wissenschaftsparks Albert Einstein on November 20, 2013

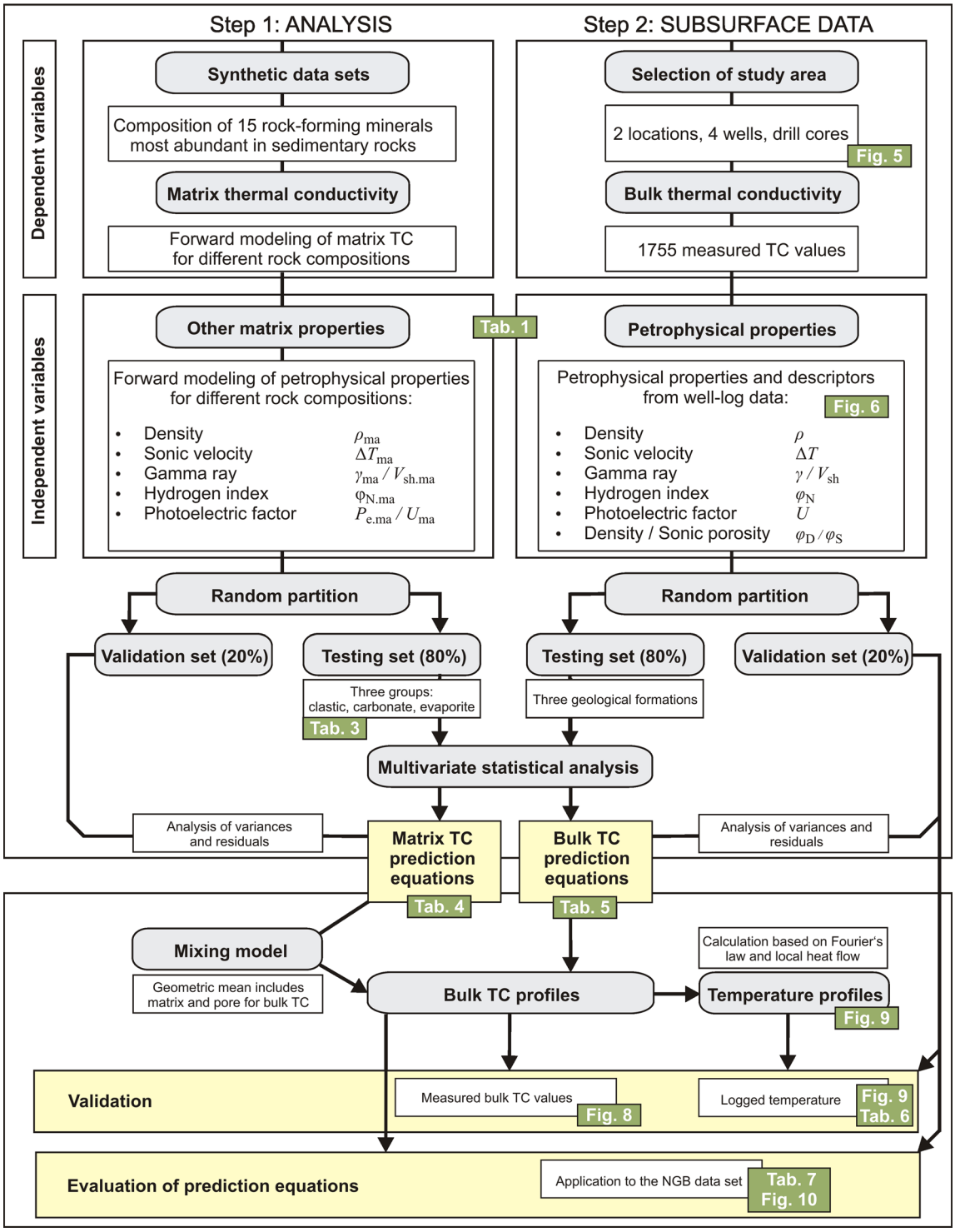

Figure 1. Workflow for TC prediction from petrophysical properties of sedimentary rocks.

3 METHODS

3.1 Workflow

Considering the limitations that past studies have shown in the well-log based prediction of TC, we have selected a different approach whose workflow is provided in Fig. 1. In a first step, for large sets of mineral assemblages it is studied how the TC of the most typical rock-forming minerals of sediments is correlated with individual, conventional petrophysical well-log properties and how these correlations are influenced by an assumed porosity. Matrix TC prediction equations are derived, which are used to calculate bulk TC based on porosities from well logs. In a second step, prediction equations for bulk TC are developed using a set of conventional petrophysical well logs and measured TC values from the Mesozoic section of the NGB. The most accurate prediction equations in turn are used to calculate TC profiles for full borehole sections. The calculated TC profiles are validated by comparison with measured TC and by

Downloaded from http://gji.oxfordjournals.org/ at Bibliothek des Wissenschaftsparks on November 20, 2013

Table 1. Petrophysical descriptors combined with TC.

Petrophysical descriptor	Unit	Equation
Volume fraction of shale[a]	—	$V_{\mathrm{sh.GR}} = \frac{\gamma_{\mathrm{mea}}-\gamma_{\mathrm{min}}}{\gamma_{\mathrm{max}}-\gamma_{\mathrm{min}}}$
	—	$V_{\mathrm{sh.ND}} = \frac{\phi_{\mathrm{N}}-\phi_{\mathrm{D}}}{\phi_{\mathrm{N.sh}}-\phi_{\mathrm{D.sh}}}$
Density porosity[b]	p.u.	$\phi_{\mathrm{D}} = \frac{\rho_{\mathrm{ma}}-\rho_{\mathrm{b}}}{\rho_{\mathrm{ma}}-\rho_{\mathrm{fl}}}$
Sonic porosity[c]	p.u.	$\phi_{\mathrm{S}} = \frac{\Delta T-\Delta T_{\mathrm{ma}}}{\Delta T_{\mathrm{fl}}-\Delta T_{\mathrm{ma}}}$
Total porosity[d]	p.u.	$\phi_{\mathrm{t}} = \frac{\phi_{\mathrm{N}}+\phi_{\mathrm{D}}}{2}$
Effective porosity[e]	p.u.	$\phi_{\mathrm{e}} = \phi_{\mathrm{t}}(1 - V_{\mathrm{sh}})$
Apparent matrix hydrogen index	p.u.	$\phi_{\mathrm{N.ma}} = \phi_{\mathrm{N}} - \phi_{\mathrm{D}}$
Apparent matrix density[f]	g cm^{-3}	$\rho_{\mathrm{maa}} = \frac{\rho_{\mathrm{b}}-(\phi_{\mathrm{t}}\cdot\rho_{\mathrm{fl}})}{1-\phi_{\mathrm{t}}}$
Apparent matrix acoustic transit time[f]	μs m^{-1}	$\Delta T_{\mathrm{maa}} = \frac{\Delta T-(\phi_{\mathrm{t}}\cdot\Delta T_{\mathrm{fl}})}{1-\phi_{\mathrm{t}}}$
Apparent photoelectric absorption index[f]	barns cm^{-3}	$U_{\mathrm{maa}} = \frac{U-(\phi_{\mathrm{t}}\cdot U_{\mathrm{fl}})}{1-\phi_{\mathrm{t}}}$

[a]Serra (1984). [b]Asquith & Gibson (1982). [c]Wyllie *et al.* (1958). [d]Doveton *et al.* (1997). [e]Dewan (1983). [f]Western Atlas (1995).

comparison of measured temperature-gradient profiles with those calculated according to Fourier's law using predicted TC values. Finally, previously published well-log based TC prediction methods are evaluated by application to our data set of measured TC values.

3.2 Well-log parameters and TC

Various well-log parameters, for example, bulk density (ρ_{b}), natural gamma-ray (γ), sonic interval transit time (ΔT), hydrogen index (neutron porosity, ϕ_{N}), photoelectric factor (P_{e}) and petrophysical descriptors for example, volume fraction of shale (V_{sh}), density porosity (ϕ_{D}), matrix density (ρ_{ma}) are important for this work. The basic well-log equations applied in this study are listed in Table 1.

In general, the total response of a geophysical tool (L_{total}) is determined by the volume fraction of different formation components (minerals and pore space with filling fluid, V_{i}) and their theoretical tool response (L_{i}) with the constraint that $\sum V_i = 1$ (eq. 1, e.g. Savre 1963; Doveton & Cable 1979; Serra 1984)

$$L_{\mathrm{total}} = \sum_1^n V_i L_i. \tag{1}$$

Thus, the total log response of any user-defined rock composition can be calculated (e.g. for ρ_{b}, U, ϕ_{N} and in the laminated case ΔT; see Savre 1963; Serra 1984). Where several radioactive minerals are present, the gamma-ray tool response is a function (eq. 2) of the concentration by the weight of *i*th mineral in the rock and the density of the rock matrix (Serra 1984):

$$GR\rho_{\mathrm{b}} = \sum_1^n \rho_i V_i A_i. \tag{2}$$

Typical log-response values of minerals and fluids, valid for ambient conditions, are listed in Table 2. If volume fractions were determined from well-log data, the KIWI-tool (Doveton 1986) was used.

Following the experience of previous authors (e.g. Woodside & Messmer 1961; Sass *et al.* 1971; Merkel *et al.* 1976; Brigaud & Vasseur 1989) the geometric mean model, originally introduced by Lichtenecker (1924), was used to calculate matrix TC (λ_{ma}, eq. 3) from the mineral constituents, as well as to calculate the saturated bulk TC (λ_{b}, eq. 4) using the matrix TC and porosity (Φ) (e.g. Fuchs *et al.* 2013):

$$\lambda_{\mathrm{ma}} = \prod_1^n \lambda_i^{V_i}, \tag{3}$$

where V_i is the volume fraction of each component,

$$\lambda_{\mathrm{b}} = \lambda_{\mathrm{ma}}^{1-\phi}\,\lambda_{\mathrm{p}}^{\phi}, \tag{4}$$

where λ_{p} is the TC of the pore-filling fluid.

3.3 Statistics

All data were randomly subdivided in two groups, one set of test data (80 per cent of data) and one set of validation data (20 per cent of total data). The test data set was used for statistical analysis, while the validation data set was used to prove the statistical quality of the deduced prediction equations (Fig. 1).

SLR, MLR and NLR analysis based on a least-squares estimation were applied to predict the values on a quantitative outcome variable (dependent variable: TC) using one or more predictor variables (independent variable: well-log values). Levels of 'F to enter' and 'F to remove' were set to correspond to p levels of 0.05 and 0.1, respectively.

The performance of the applied methods was evaluated by test (values not reported) and validation data (reported fitting data) using the arithmetic mean error (ame), the standard error of the estimate (SE), and the coefficient of determination (R^2) between predicted and measured values, respectively. SE explains the excursions of the given TC values from the computed regression line and is defined as the rms value:

$$\mathrm{rms} = \sqrt{\frac{1}{n}\sum_{i=1}^n (\mathrm{TC}_{\mathrm{mea}.i} - \mathrm{TC}_{\mathrm{pred}.i})^2}, \tag{5}$$

where n is the number of samples.

R^2 describes the dependent-variable variance (TC), which is explained by the independent-variable variance (log-response values). In this study, the adjusted R^2 value is reported, which is frequently slightly smaller than R^2, but more robust by taking into consideration the number of observations and the number of predictor variables. Coefficient of variation (cv) is given as the quotient of rms value and arithmetic mean value of the measured TC. Coefficient of variation values <10 per cent are assumed as an indicator for a valid prediction model. All prediction equations developed and presented hereafter show an acceptable level of multicollinearity (tolerance > 0.3), which means a low level of correlation between two predictor variables, and the standardized residuals are always (nearly) randomly distributed.

Downloaded from http://gji.oxfordjournals.org/ at Bibliothek des Wissenschaftsparks Albert Einstein on November 20, 2013

Table 2. Petrophysical properties and logging-tool characteristic readings of rock-forming minerals typical in sedimentary rocks and of fluids.

Class	Name	Abbreviation	TC [W (m K)$^{-1}$]	ρ (g cm^{-3})	U (barns cm^{-3})	Φ_N (p.u.)	ΔT (μs m^{-1})	γ (API)
Carbonates	Dolomite	Dol	5.4[a,b,c,d]	2.88[e]	9[e]	0.02[e]	140[e,f]	0[a]
	Calcite	Cal	3.4[a,b,c,d]	2.71[e]	13.77[e]	0[e]	153[e]	0[e]
Clays	Kaolinite	Kln	2.7[a,b]	2.42[e]	6.17[e]	0.37[e]	211[g]	80[e]
	Montmorillonite	Mnt	1.85[a,b]	2.12[e]	4.3[e]	0.12[e,g]	212[g]	150[e]
	Illite	Ilt	1.8[a]	2.75[e,h]	11.05[e]	0.2[e]	211[g]	250[e]
Feldspats	Orthoclase	Or	2.25[a,b,c]	2.57[h]	7.5[e]	–0.02[e]	233[e]	220[e]
	Albite	Ab	2[c]	2.62[e]	4.35[e]	–0.01[e]	165[e,f,g]	0[e]
	Anorthite	An	1.9[b]	2.74[e]	8.58[e]	–0.02[e]	145[c]	0[e]
Hallogenides	Sylvite	Syl	8.5[b]	1.98[e]	15.83[e]	–0.02[e]	242[g]	747[e]
	Halite	Hl	6.5[c]	2.15[e]	9.48[e]	–0.02[e]	229[e]	0[e]
Micas	Muscovite	Ms	2.33[c,f]	2.82[e]	7.33[e]	0.185[e,g]	151[e,f,g]	270[e]
	Biotite	Bt	2[c]	3[e]	19.8[e]	0.21[e]	195[f]	200[e]
Oxides	Quartz	Qz	7.7[a]	2.65[e]	4.79[e]	–0.02[e]	182[e]	0[e]
Sulfates	Anhydrite	Anh	4.8[b,c,d]	2.96[e]	14.93[e]	–0.02[e]	164[b,e,g]	0[e]
	Gypsum	Gp	1.3[e]	2.32[e]	9.37[e]	0.49[e]	174[d]	0
Fluid	Air		0.025[i]	0.0012	–	0	3021[b]	–
	Water		0.604[j]	1.15	0.96	1.05	620[e]	–
	Oil		0.14[b]	0.88[e]	0.11[e]	–0.02	770[e]	–

[a]Serra (1984); [b]Brigaud & Vasseur (1989); [c]Fertl & Frost (1980); [d]Schön (1996); [e]Schön (1983); [f]Horai (1971); [g]Čermák & Rybach (1982); [h]Lemmon *et al.* (2005); [i]Crain (2013); [j]Gröber *et al*. (1955). Mineral abbreviations after Whitney & Evans (2010).

3.4 Pressure and temperature correction of laboratory-measured TC

The TC values predicted in this study from standard well-log parameters basically represent the physical properties of the rock matrix plus porosity. Pressure and temperature influences on the laboratory-measured TC are a priori not considered. For the validation of predicted bulk TC temperature-gradient plots from measured temperature logs are compared with respective plots calculated on the basis of predicted bulk TC and a site-typical value of surface heat flow (*cf.* Section 5.2). For this purpose, the predicted TC values are corrected to *in situ* values by applying pressure and temperature corrections.

For the correction of the temperature effect the equation of Somerton (1992) is used. The pressure correction was made with a new equation that is based on various relations derived from laboratory experiments on sedimentary rocks (sandstone, anhydrite, greywacke, conglomerate, limestone and dolomite) and crystalline rocks (granite, amphibolite and gneiss; Fig. 2):

$$TC_{\mathrm{cor}} = (1.095 \cdot \mathrm{TC_{lab}} - 0.172) \cdot p^{(0.0088 \cdot \mathrm{TC_{lab}} - 0.0067)}, \quad (6)$$

where TC_{lab} is the zero-pressure TC in W (m K)$^{-1}$ and p is the assumed *in situ* pressure in MPa.

The pressure build-up TC values involved in the equation were obtained under different experimental conditions (e.g. uniaxial, triaxial and (quasi-)hydrostatic pressure; air, water or oil as pore-filling fluid) to maximum values of 400 MPa. With sufficient certainty, eq. (6) can be applied to laboratory TC between 1.5 and 5.0 W (m K)$^{-1}$.

4 ANALYSIS

4.1 Relations of TC and petrophysical properties of minerals

A data set was compiled, comprising TC values and logging-tool response values (ρ_b, P_e, ϕ_N, ΔT and γ) for 15 rock-forming minerals most abundant in sedimentary rocks (Table 2), to study the interrelations between TC and these parameters. Fig. 3 shows that the interrelations between the different petrophysical properties and TC differ largely. The TC-density plot (Fig. 3a) for example is highly diffuse; no global trend is apparent. Carbonate minerals show a positive correlation with TC, which continues with increasing content of clay (e.g. the carbonate-mudstone facies), except of illite. Clastic rocks, composed of quartz, mica, plagioclase and illite are negatively correlated with TC; whereas rocks composed of quartz, orthoclase, montmorillonite and kaolinite show a weak positive correlation, respectively. The nonexistence of a unique global TC–density correlation is in contradiction to the results of Horai & Simmons (1969), who recognized a correlation for minerals with the same mean atomic weight. Application of a regression equation formulated by Schön (1996) based on the database of Horai and Simmons did not reproduce any TC for the 15 rock-forming minerals used in this study. The difference to our results may be explained by the fact that Horai and Simmons included in their database of 119 minerals also those that are not regarded as typical rock-forming minerals of sedimentary rocks.

The interrelation between TC and sonic transit time (Fig. 3b) is well described by the Debye theory and the Birch relationship (Birch 1960, 1961). Horai & Simmons (1969) determined a positively correlated trend from the data of Birch (1960, 1961) and Simmons (1964a,b). However, this trend cannot be observed for all minerals included in this study. A negative correlation can be observed within halogenides, while a positive correlation can be observed in the carbonate–mudstone system. For clastic rocks, the correlation trend largely depends on the most abundant mineral after quartz.

The TC–photoelectric factor plot (Fig. 3c) shows a similarly diffuse scatter as the TC versus density and sonic transit time. However, P_e, ρ_b and ΔT are suitable for the separation between evaporites, carbonates and clastic rocks.

A clear nonlinear trend is observed between TC and the hydrogen index obtained from the ϕ_N-log (Fig. 3d). Halogenides, feldspars, carbonate minerals and anhydrite comprise the entire spectrum of TC values, but show only low hydrogen-index values. Only OH-bearing sheet silicates (e.g. clay minerals, micas and gypsum), exhibit a moderate or high hydrogen index (corresponding with low TC values). Thus, TC prediction from the hydrogen-index values alone is for most of the minerals impossible.

Downloaded from http://gji.oxfordjournals.org/ at Bibliothek des Wissenschaftsparks on November 20, 2013

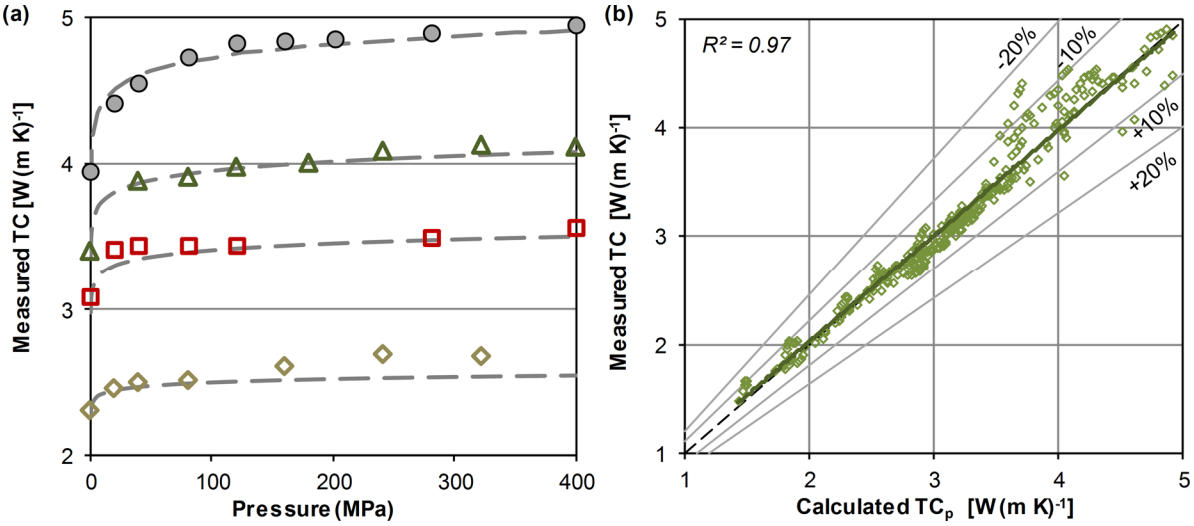

Figure 2. Pressure dependence of rock TC. (a) Laboratory measured TC as function of pressure for selected lithotypes (dot: anhydrite, open triangle: dolomite, open rectangle: limestone, open diamond: sandstone). Dashed lines are calculated from eq. (6). Eq. (6) originated from data by Woodside & Messmer (1961), Walsh & Decker (1966), Hurtig & Brugger (1970), Balling *et al*. (1981), Buntebarth (1991), Seipold & Huenges (1998), Abdulagatova *et al*. (2009) and Abdulagatova *et al*. (2010). (b) Measured versus calculated (eq. 6) TC.

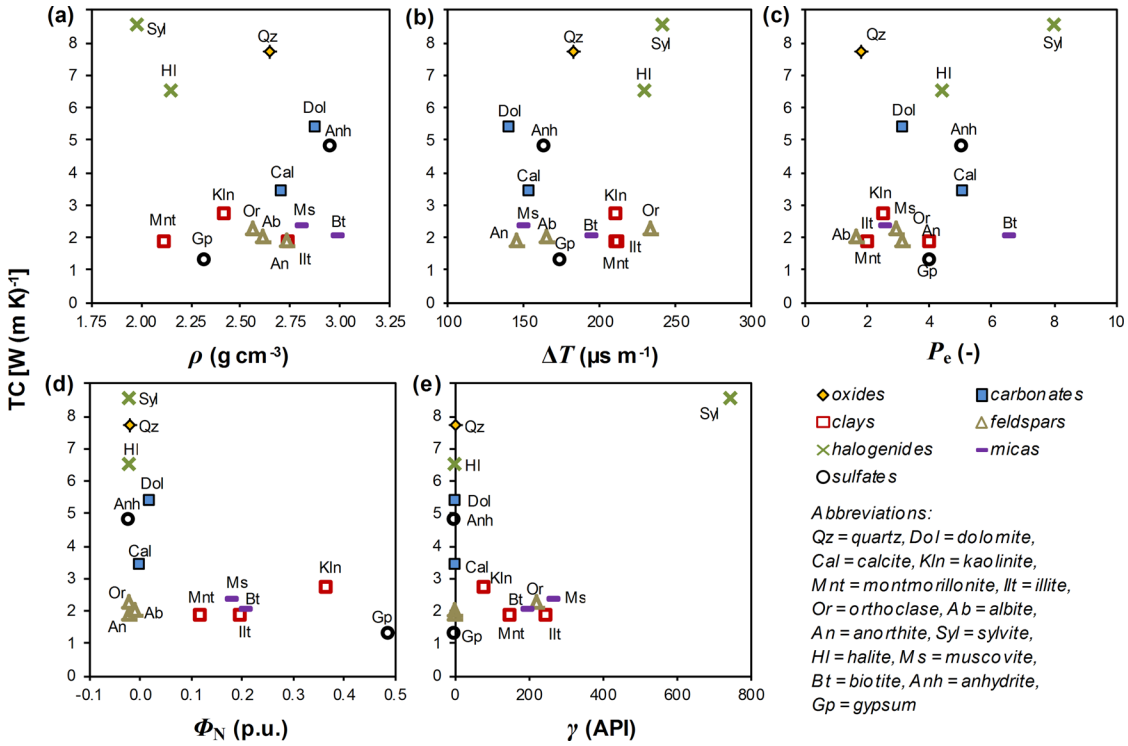

Figure 3. TC versus petrophysical properties for 15 rock-forming minerals common in sedimentary rocks. Plotted mineral data are from Table 2.

The gamma-tool response values are completely uncorrelated (Fig. 3e) to TC. However, it is remarkable that the most gamma-active minerals (clay minerals, mica, alkali feldspar) show TC values in a narrow range [between 1.5 and 3.0 W (m K)$^{-1}$]. Owing to this, incoherent negative correlations between TC and gamma ray can be observed in quartz-dominated sediments. However, obviously this cannot be regarded as universally valid.

The TC prediction capability of all five predictor variables is poor [best case using MLR: Adj. $R^2 = 0.26$, rms = 2.02 W (m K)$^{-1}$], which is no surprise. Changes of correlation trends within or between formations of different composition have a crucial impact on the prediction results, if empirically equations with fixed regression coefficients are used. Those regression coefficients are equal to the slopes for the different predictor variables, indicating the correlation trends between dependent and independent variable. The final predicted TC value is cumulative from the partial TC values coming from each (input) predictor variable. The resulting misfit coming from these trend changes results in a high inaccuracy

Downloaded from http://gji.oxfordjournals.org/ at Bibliothek des Wissenschaftsparks Albert Einstein on November 20, 2013

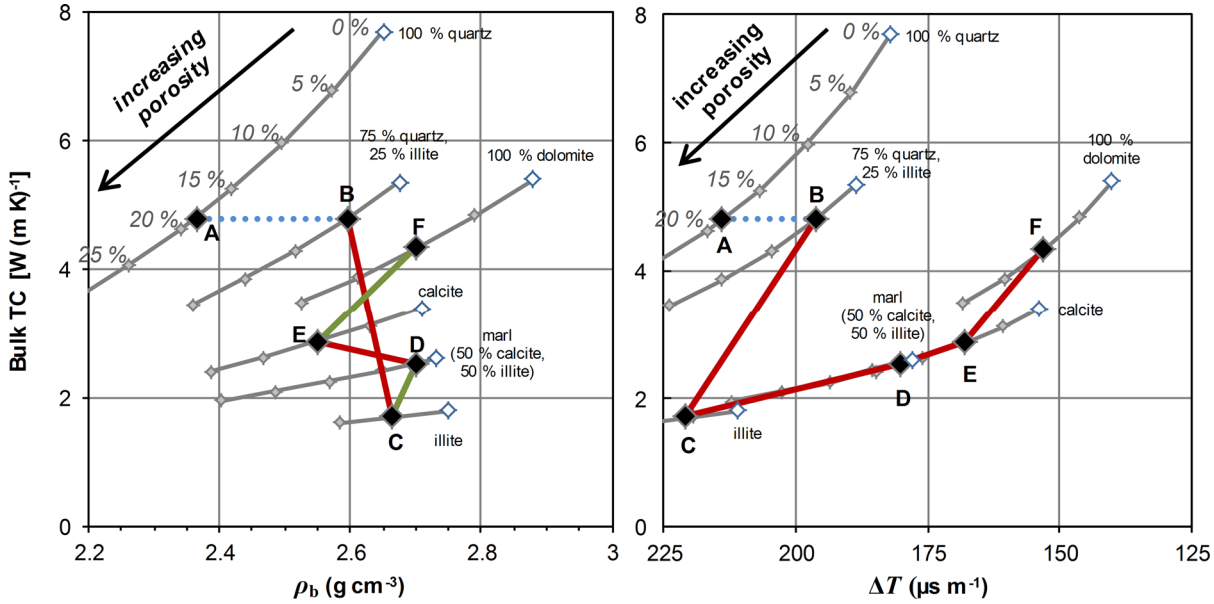

Figure 4. Influence of rock porosity on the correlation trends for two-component systems (matrix minerals and porosity). Black diamonds: (A) sandstone (matrix: 100 per cent quartz; 18 per cent porosity), (B) shaly sandstone (matrix: 75 per cent quartz, 25 per cent illite; 5 per cent porosity), (C) claystone (matrix: 100 per cent illite; 5 per cent porosity), (D) mudstone (matrix: 50 per cent calcite, 50 per cent illite; 3 per cent porosity), (E) limestone (matrix: 100 per cent calcite; 10 per cent porosity), (F) dolomite (matrix: 100 per cent dolomite; 10 per cent porosity). Blue dotted line: no correlation, red line: negative correlation, green line: positive correlation.

in SLR, which can possibly, at least partly, be compensated using additional predictor variables in explanation of TC (using MLR). However, such simultaneous change of predictor variables poses an increased danger of multicollinearity for MLR techniques and, therefore, instable estimates for the coefficients. Thus, the major correlation trends are of great importance for the use of regression techniques.

Curve fitting with NLR or the application of ANN techniques (feedforward backpropagation neural networks) provides no better fit than MLR. Obviously, there is no fundamental relationship between TC and other petrophysical properties that could be obtained for the selected rock-forming minerals. Some pairs of petrophysical properties are clearly uncorrelated, while others show only poor correlations. Thus, it is fair to assume, that in some situations other factors must have influenced the relationships observed by various authors on rock samples. Porosity and the type of pore-filling fluid (e.g. water, air, oil and gas) are obvious factors.

4.2 Influence of porosity on the relations of TC and petrophysical properties of rocks

The total log response significantly changes with different porosity because of the contrast in properties of the pore-filling fluid compared to those of the matrix mineral grains (Table 2). This fact is well displayed in the cross-plots for different two-component (matrix mineral and porosity) systems, exemplarily shown for ρ_b and ΔT (Fig. 4). Depending on the TC value of the matrix component, different porosity values result in different slopes and slope directions (correlation coefficients). Those changes in correlation trends (positive or negative correlations) imply problems for regression techniques as previously described. For example, the change from a clay-free 'quartz rock' (representative of clean sandstone) of high porosity to a quartz-illite mixture (argillaceous sandstone) result in positive correlations between TC and density whereas negative correlations can be expected for a low-porous 'quartz rock' (Fig. 4a). The same effect can be observed for numerous other lithotype combinations. In contrast, the TC–ΔT relation, exemplarily shown in Fig. 4(b), indicates only negative correlations. In conclusion, due to the ambiguous influence of porosity on the correlation trends we proceed in the TC prediction with the focus on the mineral constituents of the rock matrix and thus the matrix TC.

4.3 Matrix-TC prediction for artificial rock compositions

For this purpose, the sedimentary rocks are classified into three major groups (I) carbonates, including mudstones, (II) clastic rocks and (III) marine evaporites (Table 3). For the groups (I) and (II), multimineral rock compositions are defined, based on the stepwise combination (in 10 per cent steps) of different rock-forming minerals common in sedimentary rocks. This procedure is performed as long as each mineral was combined with each other within the limitations defined in Table 3. For the group (III), the marine evaporites, an artificial data set of rock composition is generated by stepwise combination of two minerals of the calcite–dolomite–gypsum–anhydrite–halite–potassium–magnesium–salt sequence.

Petrophysical properties are calculated for each mineral combination shown in Table 3 using the mineral data given in Table 2, which in turn formed the basis for the prediction equations of matrix TC. Thus, for rocks with the same mineralogy, the matrix well-log response, computed from the bulk tools response and the porosity (applying eqs 1, 2 and 4, and typical log-response values from Table 1), should be equal to the petrophysical properties calculated for this mineralogy. Prediction equations for matrix TC are calculated by using multiple regression analysis. Taking into account the balance between the use of as few as possible different well logs and the need to achieve a large explained variance (minimizing the prediction error), the 'optimal log configuration' for each rock group and the deduced empirical relationships are described in the following subsections. However, in many cases the 'optimal log configuration' for determination of matrix TC is not available,

Downloaded from http://gji.oxfordjournals.org/ at Bibliothek des Wissenschaftsparks on November 20, 2013

Table 3. Groups of sedimentary rocks with respect to their assumed rock composition, and the min-max range of the particular minerals.

Group	Mineral	Range		
		Carb. (per cent)	Clast. (per cent)	Evap. (per cent)
Oxides	Quartz	0–50	50–100	—
	Anorthite	—	0–50	—
Feldspars	Albite	—	0–50	—
	Orthoclase	—	0–50	—
Micas	Muscovite	—	0–20	—
	Biotite	—	0–20	—
	Kaolinite	0–70	—	—
Clays	Montmorillonite	0–70	0–100	—
	Illite	0–70	0–100	—
Carbonates	Calcite	0–100	0–20	0–100
	Dolomite	0–100	0–20	0–100
Sulfates	Anhydrite	—	0–20	0–100
	Gypsum	—	—	0–100
Chlorides	Halite	—	—	0–100
	Sylvite	—	—	0–100

Note: Carb., carbonates; Clast., clastic rocks; Evap., evaporites.

Table 4. Matrix-TC equations derived from regression analysis for major sedimentary rock types.

Rock group	Matrix TC prediction equations	R^2	n	rms [W (m K)$^{-1}$]	ame (per cent)	SD (per cent)	cv (per cent)	T	F	B_{s1}	B_{s2}	B_{s3}	eq.
Evaporites	$\lambda_m = 14.06 - 10.35\phi_{N.ma} - 3.37\rho_{ma}$	0.92	51	0.45	7.0	5.6	8.8	0.99	237.4	–0.81	–0.50	—	(7)
Carbonates	$\lambda_m = 5.058 - 0.1\rho_{ma} - 2.915V_{sh}$	0.95	2252	0.17	4.2	3.2	5.1	0.38	14891	0.46	–0.79	–0.67	(8)
	$\lambda_m = 3.093\rho_{ma} - 2.727V_{sh} - 0.332U_{ma} - 0.55$	0.7	2252	0.39	9.2	6.8	10.6	0.58	2653	–0.15	–0.85	—	(9)
Clastics	$\lambda_m = 5.281 - 2.961\phi_{N.ma} - 2.797V_{sh}$	0.43	3484	0.44	11.4	9.1	14.7	0.55	1336	–0.58	–0.11	—	(10)

Note: All predictor variables are highly significant ($p < 0.001$). For statistics see Section 3.3, for abbreviations see the Appendix A.

in particular in old boreholes. Then, matrix TC can be predicted by using one of the additional regression equations listed in the Appendix B. The appendix comprises regression coefficient, statistical parameters and the expected prediction errors (for artificial and subsurface data set) for each possible combination of well logs used in this study. Considering larger prediction uncertainties, this allows a TC prediction even if the required and recommended log combination is not available.

4.3.1 Carbonates

In a first attempt, all matrix well-log properties (Table 2) are included in the regression analysis (MLR). The result is a nearly perfect coefficient of regression ($R^2 = 0.98$). Considering that the largest impact on the explained variance is by the first three predictor variables, ρ_{ma}, V_{sh} and U_{ma} ($R^2 = 0.95$), a prediction equation with three variables (Table 4, eq. 8) is a proper choice if a minimal number of well logs shall be included in the TC prediction. The matrix TC is determined with an error of <10 per cent for >96 per cent of the predicted values. This is that 95 per cent of the values show deviations of <0.24 W (m K)$^{-1}$]. The implementation of U_{ma} in the prediction equation results only in a slightly improved explained variance. Furthermore, ρ_{ma} and U_{ma} show signs of multicollinearity (tolerance $\sim$ 0.3). Thus, U_{ma} could be ignored in the TC prediction if the respective log is not available. The resulting, two-predictor-equation (Table 4, eq. 9) shows no multicollinearity (tolerance > 0.5) and is able to predict >60 per cent of the values with deviations <10 per cent. This is that 50 per cent of the values show deviations of <0.25 W (m K)$^{-1}$. The coefficient of determination ($R^2 = 0.70$) is high, indicating a good degree of tracking. The prediction errors (ame, rms) are in the order of 9.2 per cent and 0.39 W (m K)$^{-1}$.

4.3.2 Clastic rocks

The high variability of ρ_{ma} and ΔT_{ma} of major clay minerals (illite, montmorillonite and kaolinite) are the main challenging factors for a valid prediction equation for matrix TC using MLR. For these properties, changes in the correlation trend from one clay mineral to another as well as from one rock composition to another (see also Fig. 3) do not allow a development of a valid empirical prediction equation for matrix TC. Even for the simplest rock matrix model, consisting of quartz and different clay minerals, the prediction failed by using the full suite of available well-log parameters. Only for rocks composed of quartz, feldspar, and mica and one clay mineral only a nearly perfect coefficient of variation is achieved. That is why ρ_{ma} and ΔT_{ma} were not taken into further consideration, and the prediction model is reduced to the use of V_{sh} and $\phi_{N.ma}$. The resulting two-predictor-equation (Table 4, eq. 10) shows no multicollinearity (tolerance > 0.55) and is able to predict >67 per cent of values with deviations of <10 or 92 per cent with deviations <20 per cent, respectively.

4.3.3 Evaporites

A stepwise MLR was performed using $\phi_{N.ma}$, U_{ma}, ΔT_{ma} and ρ_{ma} as predictor variables. Regarding that none of the considered minerals (Table 3) show an intrinsic natural gamma response, the gamma-ray log, and thus the calculated V_{sh} are no useful TC predictors for the evaporate sequence. However, they are certainly useful for a lithological identification. The $\phi_{N.ma}$ log response delivers the largest part of the shared explained variance for the predicted TC. Step 1 results in $R^2 = 0.67$. In step 2, ρ_{ma} was added as further predictor variable, which improved the result significantly to $R^2 = 0.92$

Downloaded from http://gji.oxfordjournals.org/ at Bibliothek des Wissenschaftsparks Albert Einstein on November 20, 2013

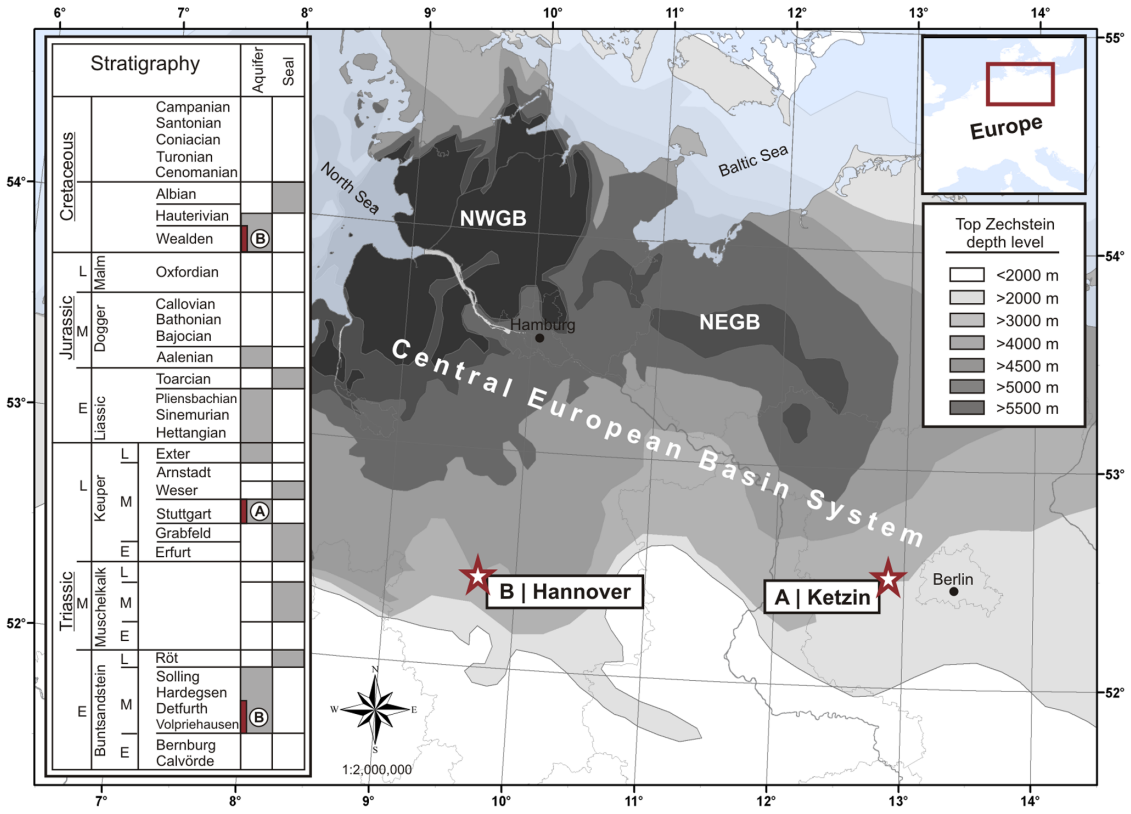

Figure 5. Studied borehole sites in the North German Basin. (A) the Ketzin site; (B) the Hannover site. NEGB, Northeast German Basin, NWGB, Northwest German Basin. Generalized stratigraphic column of the Mesozic with major geothermal sandstone aquifers and major aquitards (modified Feldrappe *et al.* 2008). Red bars indicates the section studied in this paper.

(Table 4, eq. 7). ΔT_{ma} and U_{ma} provided no further explained variance and thus were not implemented in the prediction equation. Using this equation, >80 per cent of the predicted values show deviations <10 per cent. This is that 60 per cent of values show deviations <0.25 W (m K)$^{-1}$. The ame value is in the order of 7.0 per cent.

4.4 Bulk-TC prediction from laboratory measured TC and well-log data of the NGB

For the TC prediction, well-log data were used from two sites (Fig. 5). At site A, the Ketzin site, data were available from three wells (the Ktzi 200, Ktzi 201 and Ktzi 202 boreholes) drilled to a total depth of approximately 800 m as part of the CO_2SINK project (Norden *et al.* 2010). The wells bottom in the Upper Triassic (Stuttgart Formation, Middle Keuper). At site B, the Hannover site, well-log data from the Groß-Buchholz well (GT 1) are used (Hübner *et al.* 2012; Schäfer *et al.* 2012). The well, drilled in the framework of the GeneSys project, has a total depth of approximately 3900 m and bottoms in the Lower Triassic (Middle Buntsandstein). Thus, the four boreholes represent a combined subsurface section of the whole Mesozoic in the NGB.

A total of 1755 TC values were measured under ambient laboratory conditions on drill cores retrieved from these boreholes and used in this study to develop prediction equations for bulk TC from well logs. 733 TC values (B. Norden, personal communication 2013) are from the Stuttgart Formation (~80 m thick) at the Ketzin site. The Stuttgart Formation is lithologically heterogeneous and made up of fluvial sandstones (feldspathic litharenites and lithic askoses) and siltstones interbedded with mudstones showing remarkable differences in porosity caused by high contents of anhydritic cementation in some extent (Förster *et al.* 2006, 2010; Norden *et al.* 2010). 1022 values are from the Wealden Formation (190 m thick, cored between 1208 and 1223 m) and the Middle Buntsandstein (250 m thick) at the Hannover site (Orilski *et al.* 2010). The Wealden Formation is dominated by sandy siltstones and silty claystones, which are interbedded by thin well-sorted sandstones (subarkoses and sublitharenites). Medium porosity values (10–15 per cent), low densities, and clay-mineral, carbonate and silicaceous cementation were commonly observed (Hesshaus *et al.* 2010; Hübner *et al.* 2012). Middle Buntsandstein samples from this site are dominated by carbonate and anhydrite cemented, fine- to medium grained, well-sorted sandstones of low porosity (<3 per cent; Röhling & Heinig 2012), siltstones and claystones (Hesshaus *et al.* 2010), respectively. On both locations, the neutron porosity was logged as limestone porosity.

For the Ketzin site, measurements of water-saturated bulk TC (n = 733) on drill-core samples were performed by B. Norden (personal communication, 2013). For the Hannover location, bulk TC was measured (n = 1022) on dry drill-core samples by Orilski *et al.* (2010). Both sets of TC data were obtained under ambient conditions (T ~ 293 K; atmospheric pressure) using the high-resolution optical scanning method developed by Popov *et al.* (1999). The dry measured TC data from the Hannover location were converted to water-saturated bulk TC using well-log derived porosity and the corrected geometric mean model (Fuchs *et al.* 2013).

Downloaded from http://gji.oxfordjournals.org/ at Bibliothek des Wissenschaftsparks on November 20, 2013

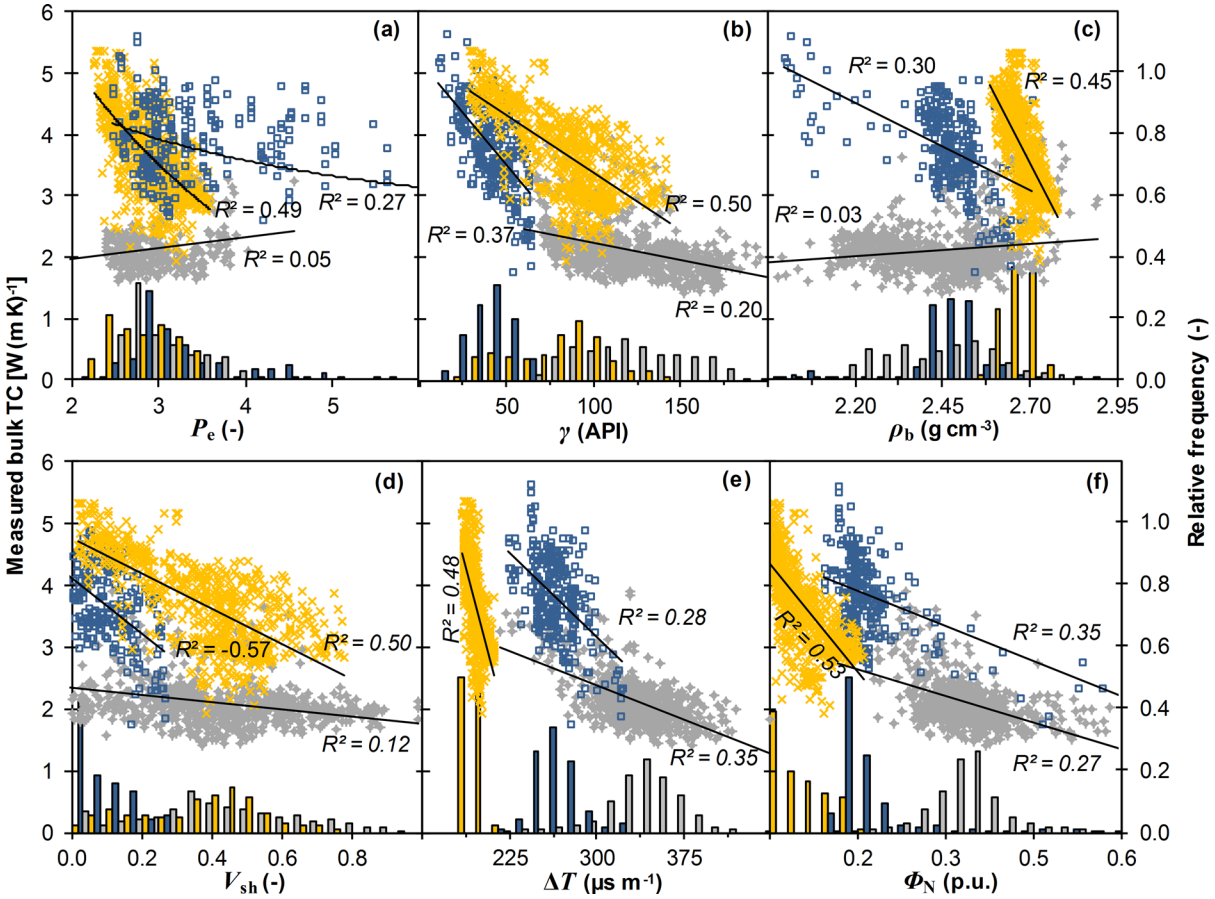

Figure 6. Cross-plots of well-log data and measured bulk TC (y-axis on the left) for the NGB data set. Colored bars (histogram) represent the relative frequency (y-axis on the right) of the petrophysical property values. R, Pearson's correlation coefficient. Yellow cross, Middle Buntsandstein; blue rectangle, Wealden Fm.; grey diamond, Stuttgart Fm.

The data set was analyzed for the relations of measured bulk TC and single petrophysical well-log parameters (Fig. 6). Density and photoelectric factor show different correlation coefficients for the three geological formations analyzed. TC is negatively correlated with ρ_b and P_e for the Middle Buntsandstein ($R = -0.67$ and -0.7) and weakly positive correlated for the Stuttgart Fm. ($R = 0.17$ and 0.23), respectively. For gamma ray (and thus V_{sh}), ΔT and ϕ_N only positive correlations are observed, whereby Stuttgart Fm. samples show always significantly lower correlation coefficients than the other two formations.

The data set of measured bulk TC formed the basis for development of a prediction equation of bulk TC using the petrophysical well-log properties shown in Fig. 6. This analysis was performed for the full data set on the one hand and individually for the three geological formations on the other hand.

4.4.1 *Analysis of the full data set*

A first MLR with all five predictor variables resulted in a moderate coefficient of determination of approximately 0.79. However, caused by the large number of input variables, a high level of multicollinearity was present (tolerance < 0.4), so that the model was rejected. The largest impact on the explained variance was by ϕ_N and V_{sh}. MLR including only these two variables (Table 5, eq. 11) shows a somewhat lower coefficient of determination ($R^2 = 0.75$) and a very low level of multicollinearity (tolerance $= 0.96$) compared to the five-variable model. Both the ame value [0.33 ± 0.26 W (m K)$^{-1}$] and the cv value (12.8 per cent) are acceptable. More than 70 per cent of samples show deviations <20 per cent.

4.4.2 *Analysis of Wealden formation*

A first stepwise regression analysis showed that ϕ_N, ρ_b, V_{sh} and U were useful predictor variables. However, V_{sh} and U provided only a low additional explained variance (ΔR^2: 0.041). Thus, a reduction of the regression model to ϕ_N and ρ_b (Table 5, eq. 12; Fig. 7a) results in a somewhat larger error [Δrms: 0.017 W (m K)$^{-1}$], which, however, is insignificant for applications. More than 76 per cent of samples show deviations <10 per cent and nearly all samples (98 per cent) show deviations <20 per cent.

4.4.3 *Analysis of Stuttgart formation*

The most accurate bulk-TC prediction using MLR was obtained by using V_{sh}, ϕ_N and ΔT as predictor variables. The coefficient of determination ($R^2 = 0.53$) indicated a good degree of tracking (Table 5, eq. 13; Fig. 7b). The additional use of ρ_b and U as predictor variables would result in a statistically significant improvement of the prediction quality, which, however, is insignificant for applications. The average error [ame: 0.16 ± 0.15 W (m K)$^{-1}$] is low,

Downloaded from http://gji.oxfordjournals.org/ at Bibliothek des Wissenschaftsparks Albert Einstein on November 20, 2013

Table 5. Bulk-TC equations derived from regression analysis for subsurface data.

Data set	Bulk TC prediction equations	R^2	n	rms [W (m K)$^{-1}$]	ame (per cent)	SD (per cent)	cv (per cent)	T	F	B_{s1}	B_{s2}	B_{s3}	eq.
Full data set	$\lambda_b = 4.75 - 4.19\phi_N - 1.81V_{sh}$	0.75	1755	0.43	11	9.9	13	0.9	2024	–0.64	–0.40	—	(11)
Wealden Fm.	$\lambda_b = 4.97 - 2.24V_{sh} - 1.87\phi_N$	0.65	288	0.33	6.8	5.3	8.7	0.7	260	–0.55	–0.35	—	(12)
Stuttgart Fm.	$\lambda_b = 4.05 - 0.48V_{sh} - 2.06\phi_N - 0.003\Delta T$	0.53	325	0.28	9.4	11	9.8	0.3	123	–0.34	–0.29	–0.26	(13)
M. Buntsandst.	$\lambda_b = 11.95 - 1.81V_{sh} - 0.038\Delta T$	0.84	734	0.25	5.5	4.1	6.7	0.6	1843	–0.58	–0.43	—	(14)

Note: All predictor variables are highly significant ($p < 0.001$). For statistics see Section 3.3, for abbreviations see Appendix A.

more than 73 per cent of samples show deviations <10 per cent and nearly all samples (96 per cent) show deviations <20 per cent.

4.4.4 Analysis of Middle Buntsandstein

Bulk density and the V_{sh} are the most important predictor variables for these samples (Table 5, eq. 14). The coefficient of determination ($R^2 = 0.83$) is high, indicating a fair degree of tracking for the full formation (Detfurth and Volpriehausen samples). The error distribution is small [ame: 0.2 ± 0.14 W (m K)$^{-1}$], resulting in cv of approximately 7 per cent. The qualitative agreement between measured and predicted values (Fig. 7c) is obvious with most of the predicted conductivities within ±10 per cent. More than 88 per cent of samples show deviations <10 per cent and nearly all samples (99 per cent) show deviations <20 per cent.

In summary, four equations for bulk-TC prediction are developed. They display different errors of determination. The application of an overall prediction equation for clastic rocks results in errors (ame) on the order of 11.2 ± 9.9 per cent. Significantly smaller errors can be achieved by the application of individual prediction equations for the specific geological formations (ame values between 5.5 ± 4.1 and 9.4 ± 10.6 per cent).

4.5 Discussion

The weak positive correlation of TC and density obtained for the Stuttgart Fm. (Fig. 6c) is in line with previous results for shaly sediments (e.g. Beziat *et al.* 1992, clay–sand mixtures; Hartmann *et al.* 2005, shaly sands and carbonates). In contrast, the strong negative correlation of TC and density observed for the clean sandstones of the Middle Buntsandstein and the interbedded sandstones of the Wealden was not previously known, but was reported for crystalline rocks (e.g. Pribnow *et al.* 1993; Kukkonen & Peltoniemi 1998; Sundberg 2002). The negative correlation trends are consistent with the theoretical models including the rock-forming minerals (Fig. 3a). Thus, given the ambiguity in the observed trends for different rock types, the density does not seem to be a useful discriminator for clastic rocks to overcome the known limitations of previously published equations.

The weak to strong negative correlations of TC with sonic sonic interval transit time (Fig. 6e) and, vice versa the positive correlation with sonic velocity, observed for shaly sediments and low-porosity sandstones support previous observations (e.g. Sahlin & Middleton 1997; Hartmann *et al.* 2005; Goutorbe *et al.* 2006; Gegenhuber & Schön 2012). They also correlate with the theoretical observations presented in this study (Fig. 4b). However, the wide range of negative correlations caused by porosity hinders the use of this well-log parameter as a predictor variable for clastic rocks. Therefore, it is expected that most of the approaches published in literature using ΔT as a predictor variable (Table 7) will not work for our data set, especially if the standardized beta-coefficient for ΔT from MLR analysis is large.

The weak to strong negative correlations of TC with V_{sh} observed on the full data set (Fig. 6d) are generally comparable to the results of Brigaud & Vasseur (1989), who obtained similar results for sandstones of variable clay content. Also the TC–V_{sh} data scatter of the Ketzin samples and of the shaly rocks of Sahlin & Middleton (1997) are similar. Sahlin & Middleton (1997) found no obvious prediction trend for bulk TC for shales and claystones, which they explained by the large range of TC of clay minerals. On the contrary, V_{sh} is important for each of the deduced bulk-TC equations in this study (eqs 11–14) and for matrix TC calculated for clastic and carbonate rocks (eqs 8–10), respectively.

The negative correlation between TC and ϕ_N (Fig. 6f) has not yet been widely discussed in the literature. As the analysis of the (matrix) TC–ϕ_N interrelation indicates a nonlinear behavior for the group of major minerals itself, quartz-dominated rock compositions consistently generate this range of negative correlations.

The photoelectric factor was suggested by many authors (e.g. Doveton *et al.* 1997; Sahlin & Middleton 1997; Goutorbe *et al.* 2006) to be a valuable predictor variable. Our observation however delineate both positive and negative correlations with TC (Fig. 6a) making it questionable to include this variable into prediction equations for clastic rocks. In addition, following Fig. 3c, the correlation between TC and P_e in carbonate–mudstone systems strongly depends on the major carbonate and clay minerals, respectively. All in all, P_e may be more useful for the discrimination between the major depositional groups than as predictor variable in MLR analysis.

In general, different types of electrical resistivity logs are commonly available in deep wells. Thus, the implementation of this petrophysical property would be an attractive option to enlarge the application range of the proposed method. However, the method presented herein based on reliable and largely invariant log-response values of the selected minerals. Following the data of Serra (1984), that cannot be assumed for the most important minerals selected in this work (*cf.* the large resistivity range of quartz, calcite and halite, respectively). Depending on the chosen reference value the correlation of matrix resistivity with matrix TC might be positive, negative or neutral for the same composition. Thus, resistivity log was not considered in this study.

5 VALIDATION

5.1 Comparison of measured and calculated TC data

The validation of the prediction equations for TC of clastic rocks by comparison of calculated and measured TC values is made on the validation data set (Fig. 1). Matrix TC values are calculated from eqs (8) and (10) (Table 4) for carbonates and clastic rocks and transposed to water-saturated bulk TC using the geometric mean model (eq. 4) and log values of effective porosity. In addition, bulk

Downloaded from http://gji.oxfordjournals.org/ at Bibliothek des Wissenschaftsparks on November 20, 2013

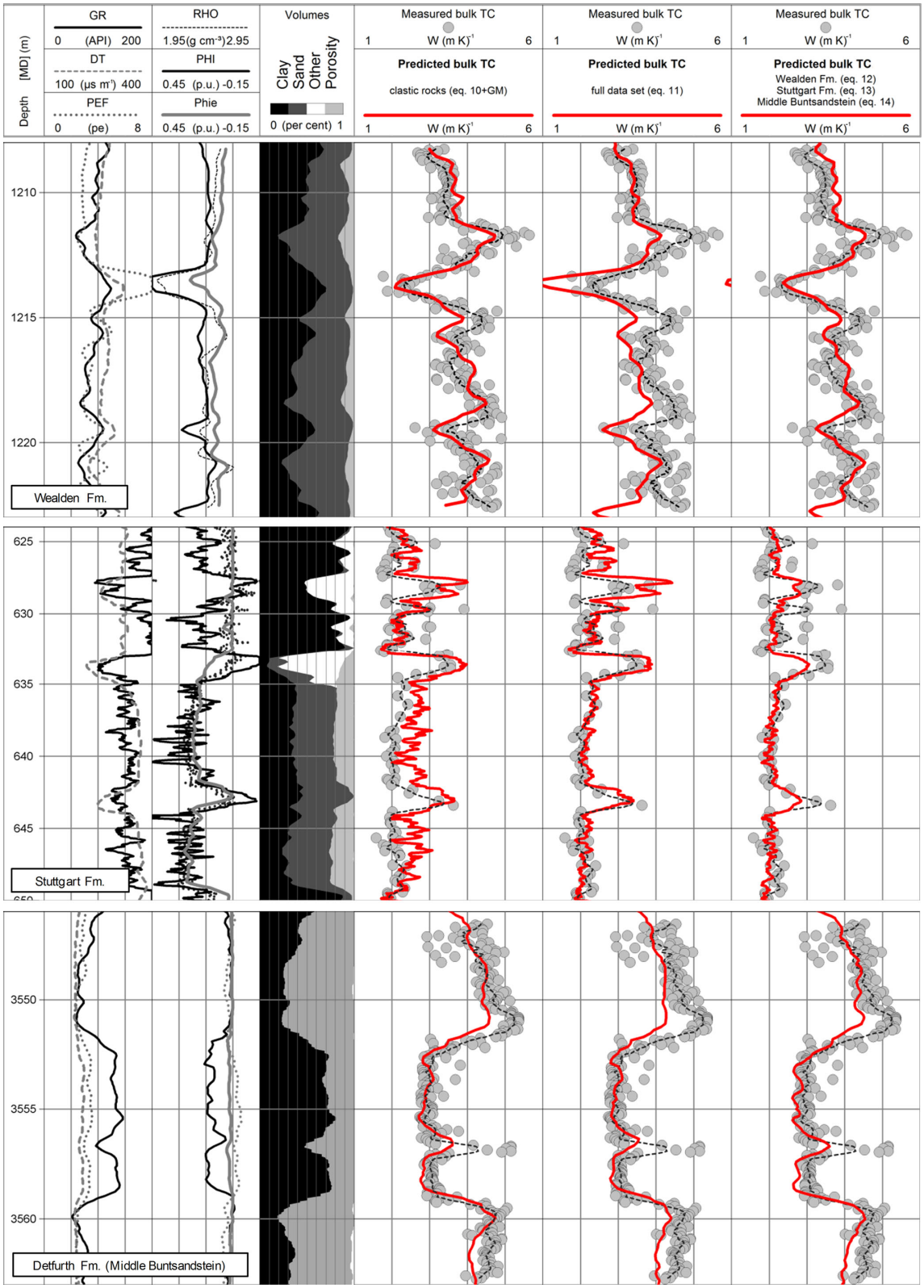

Figure 7. Comparison of well-log based TC (three right tracks). Predicted bulk TC (red line) versus laboratory-measured bulk TC (measured values: grey dots, moving average (1 m): dashed line) for three selected well sections. For abbreviations see Appendix.

Downloaded from http://gji.oxfordjournals.org/ at Bibliothek des Wissenschaftsparks Albert Einstein on November 20, 2013

TC values are calculated using eq. (11) (developed for clastic rocks independent of rock type) and using eqs (12)–(14) (developed for single rock types/geological formations).

In general, the calculated TC values mimic very well the trends of TC changes along geological sections (Fig. 7). Bulk TC calculated from eq. (13) for the Stuttgart Fm. match well measured bulk TC, but slightly overestimate those layers exhibiting a low hydrogen index. The quantification of error (Fig. 8) shows that the misfit due the hydrogen index (deviations of >50 per cent) pertains only to <8 per cent of the data. Bulk TC values calculated from eq. (11) slightly underestimate measured TC in the Wealden Fm. especially in the layers with high hydrogen index values. The rms value of the bulk TC values predicted by eqs (10)–(14) for sections shown in Fig. 7 (full data set) is between 0.24 and 0.41 W (m K)$^{-1}$. This error is comparable to the values noted by Hartmann *et al.* (2005). The lowest rms value was achieved for the Middle Buntsandstein [eq. (14): 9.8 per cent; eq. (10): 7.8 per cent] of homogeneous composition and the highest for the heterogeneous Stuttgart Fm. [eq. (13): 12.5 per cent; eq. (10): 28 per cent], respectively.

Although it was originally assumed that empirical equations for the calculation of TC are valid only for the geological formations for which they were determined (e.g. Goss & Combs 1976; Evans 1977; Molnar & Hodge 1982; Blackwell & Steele 1989; Hartmann *et al.* 2005), the results from using eq. (10) (Fig. 7) seem to be valid for all formations analyzed in this study. This can be explained by the use of an artificial data set for model development. Thus it is likely to assume that eq. (10) also can be successfully applied for any clastic rock. The use of such an artificial data set in combination with MLR is different to other approaches (e.g. Goutorbe *et al.* 2006), which favor nonlinear techniques such as neural networks as ultimate technique for 'universal' TC estimations.

The validation of the matrix TC equation for carbonates was made against the Doveton *et al.* (1997) data. The data set consists of matrix values for density and sonic transit time, gamma ray and calculated total porosity as well as bulk TC (originally published by Blackwell & Steele 1989). The ame value between measured and predicted bulk TC is 22 ± 13 per cent (eq. 9), which is comparable to the error (ame: 19 ± 16 per cent) that would stem from the application of the Doveton *et al.* (1997) TC prediction equation. Both error estimates are acceptable, given the uncertainties linked with the original data (TC measurements on cuttings using the chip technique described by Sass *et al.* 1971, sampling in 10-ft intervals, log-depth matching, upscaling, etc). Indeed, significantly smaller prediction errors could be achieved if eq. (9) would be applied to a data set of higher quality.

For both equations, ρ_{ma} and V_{sh} have the largest impact on TC prediction in carbonate-shale systems. All in all, more data would be useful to further verify prediction equations developed in this paper for both carbonate and evaporite rocks.

5.2 Comparison of measured and calculated temperature profiles

The value of any predictive TC equation must be based on its ability to reproduce the thermal characteristics of a section logged by a high-resolution temperature device to within an acceptable error tolerance (Doveton *et al.* 1997). We assume that an acceptable error would be on the order of <5 per cent, which is <1.5 K km^{-1} for an average temperature gradient of 30 and <2 K km^{-1} for a gradient of 40 K km^{-1}, respectively.

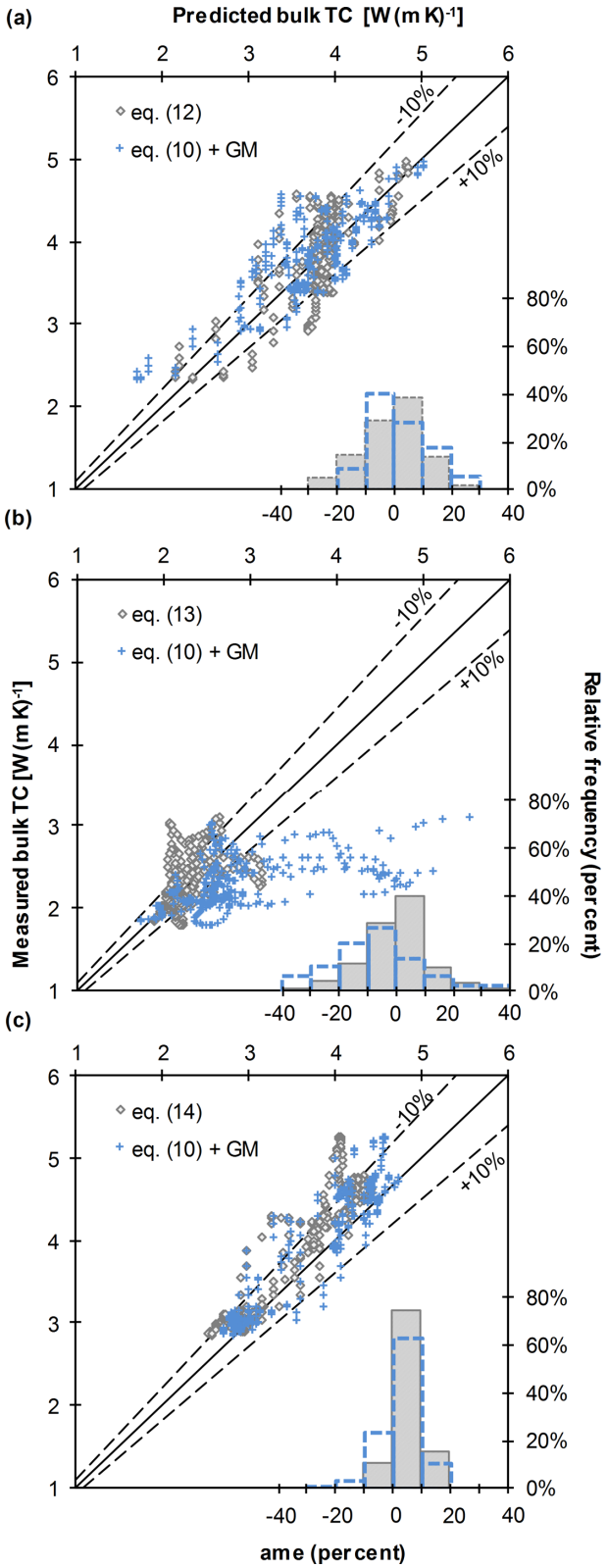

Figure 8. Scatter plots of predicted versus measured bulk TC. (a) Wealden Fm., (b) Stuttgart Fm. and (c) Middle Buntsandstein. The histogram shows the distribution (right *y*-axis) of percent errors (lower *x*-axis) between measured and predicted bulk TC [crosshatched bars; eqs (12)–(14), see Table 5] and for combination of theoretically derived matrix TC equations and geometric mean [dashed-bordered, unfilled bars; eq. (10), see Table 4].

Downloaded from http://gji.oxfordjournals.org/ at Bibliothek des Wissenschaftsparks in on November 20, 2013

For both borehole locations in the NGB (Fig. 5), high-precision temperature logs are available (Hannover location: Orilski *et al.* 2010) that are processed as temperature–gradient plots and compared with temperature gradients calculated from predicted TC. The temperature logs were measured at 0.01 m recording intervals; the logging systems had a precision of 0.001 K. The logs were obtained at least 1 yr after borehole completion, and thus are regarded as to reproduce thermal borehole equilibrium.

For the calculation of full borehole TC profiles a differentiation between various types of sedimentary rock into evaporite, carbonate, and clastic rock is made using standard lithology mapping techniques (e.g. Asquith & Gibson 1982; Serra 1984). *In situ* bulk TC then is calculated according to eqs (7), (8) and (10). In addition, the universal equation (eq. 11) is applied to intervals of clastic rock. The computation was performed for borehole sections of ∼630 m length at the Ketzin location and of ∼1.7 km length at the Hannover site. The predicted TC values are corrected for *in situ* temperature and pressure.

The predicted TC profiles are used together with a site-specific value of surface heat flow to calculate temperature-gradient profiles according to Fourier's law of heat conduction (eq. 15):

$$grad\,T = \frac{q}{\mathrm{TC}}, \tag{15}$$

where *gradT* is the temperature gradient, q is heat flow and TC is thermal conductivity.

For the Ketzin site a heat-flow value of 70 mW m^{-2} was determined using measured laboratory values of TC that were pressure and temperature corrected. For the Hannover site, a value of 82 mW m^{-2} was used (Orilski *et al.* 2010).

The theoretical temperature-gradient plots for the two sites fully reflect the lithological pattern changes of the sedimentary succession. There is also a good agreement in absolute values between measured and calculated temperature-gradient plots. At the Hannover site, differences in the temperature gradients obtained for the four intervals (Middle Keuper: 2460–2540 m, Middle Muschelkalk: 2960–3040 m, Upper Buntsandstein: 3165–3250 m, Middle Buntsandstein: 3440–3590 m) are on the order of <2 K km^{-1} (Fig. 9). For the Ketzin site, similar results are observed (Table 6). The maximum difference in absolute temperature (measured versus calculated, Fig. 9) on both sites is <0.8 and <1.3 K. This yields an average error in absolute temperature of 2.4 per cent (Hannover location) and 5.8 per cent (Ketzin location). The error is within the threshold of accepted prediction accuracy.

6 EVALUATION OF PREVIOUS APPROACHES

None of the previously published prediction equations seems to be valid universally for all types of sedimentary rocks. As the last comprehensive comparison work in this field dates back to Goss & Combs (1976) and the current state of knowledge on the applicability and prediction quality of other data sets is poor, it is timely to evaluate in this work the validity of the available prediction equations on a defined data set comprising clastic rock of the NGB.

Owing to the results of theoretical analysis performed in this paper, SLR equations considering just one predictor variable were excluded from the evaluation. Also excluded are those equations that have not fully disclosed the regression coefficients (e.g. Sahlin & Middleton 1997; Goutorbe *et al.* 2006), equations in which matrix

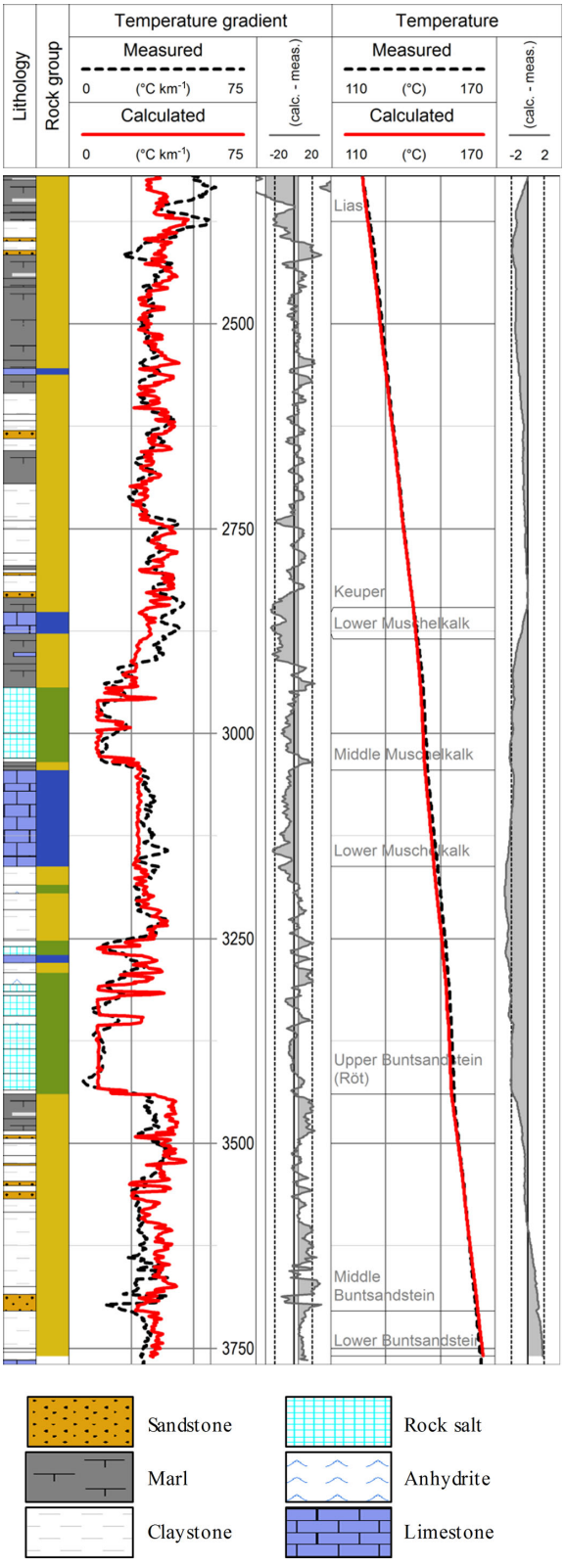

Figure 9. Comparison of measured and calculated temperature and temperature gradients. Depth in metres. Lithology is from drill core and cutting analysis as well as from well-log interpretation. Rock-group classification is a simplification of lithology consisting of clastic (yellow), carbonate (blue) and evaporites (green).

Downloaded from http://gji.oxfordjournals.org/ at Bibliothek des Wissenschaftsparks Albert Einstein on November 20, 2013

Table 6. Comparison of logged and computed temperature inverted from bulk TC profiles.

Well	No.	Depth interval			Logged T			Predicted T		Error	
		Top (m)	Bottom (m)	Length(m)	Top (°C)	Bottom (°C)	Δ (°C)	Bottom (°C)	Δ (°C)	Interval (per cent)	Total (°C km^{-1})
Ketzin 200/07	1	168.0	775.0	607.0	17.12	39.68	22.56	40.99	+1.31	5.8	2.2
Groß Buchholz GT 1	1	1172.0	1363.0	191.0	69.24	76.02	6.78	75.57	–0.45	6.6	2.4
	2	1642.0	1743.5	101.5	87.05	91.07	4.02	90.27	–0.8	19.9	7.9
	3	2321.5	3748.0	1426.5	121.55	164.38	42.83	164.61	+0.23	0.5	0.2
			Total length: 1719.0 m						Mean:	4.4 per cent	1.6 °C km^{-1}

Note: Temperature was predicted starting in each interval from top downwards. $\Delta_{\text{predicted T}}$ is the difference between the bottom-logged and bottom-predicted temperature value. The intervall error was calculated as quotient of $\Delta_{\text{predicted T}}$ and $\Delta_{\text{logged T}}$. The total error was calculated as quotient of $\Delta_{\text{predicted T}}$ and the length of the depth interval.

TC values were assumed (e.g. Griffiths *et al.* 1992), and approaches, which included well logs not considered in this study (e.g. Khandelwal 2010). Thus the comparison of TC prediction includes equations from Tikhomirov (1968), Goss *et al.* (1975), Goss & Combs (1976), Evans (1977), Vacquier *et al.* (1988) and Hartmann *et al.* (2005). Equations were reformulated to SI-units if necessary and listed in Table 7. In addition, the inverse method was applied, which derives the lithology or major mineralogy of rocks from well logs (Savre 1963; Doveton & Cable 1979; Quirein *et al.* 1986), and, in turn, applies an appropriate mixing equation to calculate bulk TC for the respective lithotype using textbook TC values (e.g. Merkel *et al.* 1976; Dove & Williams 1989; Brigaud *et al.* 1990; Demongodin, *et al.* 1991; Vasseur *et al.* 1995; Midttømme *et al.* 1997; Hartmann *et al.* 2005).

Bulk TC, calculated by implementing the well-log parameters of the NGB into these approaches is compared to measured TC, and the deviations are quantified as a prediction error (Fig. 10). The smallest prediction error is achieved by using eq. (11, this study) (ame: 11 ± 10 per cent) and by applying the matrix–TC equation (eq. 13, ame: 16 ± 15 per cent) and the geometric mean model. Both equations show a similar structure by using ϕ_N and V_{sh} as predictor variables and by avoiding the problematic ρ_b and ΔT.

Agreements of less quality are achieved for the full data of clastic rock by application of the Vacquier *et al.* (1988) equation (eq. 21; ame: 20 ± 13 per cent) developed for argillaceous rocks. Eqs (20), (22) and (23) (also from Vacquier *et al.* 1988) show better agreements for selected lithotypes only. For example, eq. (20) shows valid results only for sandstone of the Middle Buntsandstein (ame: 8 ± 6 per cent), and eq. (22) for interbedded sandstone and argillaceous rock of the Wealden Fm. (ame: 15 ± 24 per cent). The observed ame values fit into the range originally provided by these authors. Surprisingly, the equation proposed to be valid for mixtures of clastic and carbonate rocks (eq. 23) completely fails on our data set.

Application of a simple inverse model, consisting of four components (clay, sand, carbonate, and porosity), on the full data set results in an ame of 20 ± 16 per cent (Fig. 10). Application of an advanced inverse model to the Stuttgart Fm., consisting of nine components derived from elemental log analysis and detailed core analysis (Norden *et al.* 2010), results in a much lower ame value of 9 ± 12 per cent. However, it is expected, that in situations of less data on the formation mineralogy and petrography, the use of such a multi-component advanced model may cause larger errors. Indeed, the quality of the predicted TC is directly related to the prediction quality of the component volume fractions (Hartmann *et al.* 2005).

The application of the approaches of Tikhomirov (1968, eq. 16), Goss *et al.* (1975, eq. 17), Goss & Combs (1976, eq. 18), Evans (1977, eq. 19) and Hartmann *et al.* (2005, eqs 24–25) show reasonable agreements (ame: <15 per cent, rms: <20 per cent) only for the low-porosity sandstone samples of the Middle Buntsandstein, but failed completely for all other litho-stratigraphical units (ame: >23 per cent, rms >30 per cent). None of these presented equations shows an acceptable match for the full data set of clastic rocks. This could result from the implementation of sonic velocity and/or bulk density into the equations as predictor variables, for which strongly varying correlations were observed for the NGB data set (Fig. 6).

7 CONCLUSIONS

(1) Standard well-log data (bulk density, natural gamma-ray, sonic interval transit time, hydrogen index and photoelectric factor) and petrophysical descriptors derived from these are obviously not able to sufficiently reflect and explain the TC variability of an artificial 'global data set' of sedimentary rocks. Thus we conclude that no universally valid TC-prediction equation can be developed with standard well-log data and regression techniques.

(2) However, a subdivision into clastic, carbonate and evaporite rocks resulted in individual equations that predict matrix TC with a high accuracy (ame: between 4 and 9 per cent). Volume fraction of shale (carbonate and clastic rocks), matrix hydrogen index (evaporite and clastic rocks) and matrix density (carbonate and evaporite) predominantly show the largest potential as predictor variable, while sonic and photoelectric factor log often provide no additional explained variance. By combining the results of these equations (eqs 7–10), entire borehole profiles can be calculated for sedimentary successions with an error on average <9.2 per cent. In this approach, knowledge of single lithotypes or mineral composition is dispensable. We recommend to use the equations (Table 4) that are fully based on matrix log-response values for predicting matrix TC of borehole profiles.

(3) The approach of using subsurface data (well logs and measured TC) restricted to clastic rocks results in a suggestion to delineate bulk TC prediction equations for different geological formations representing a typical composition of different lithotypes. Formation-specific equations show slightly smaller prediction uncertainties (ame: between 5 and 9 per cent), than the equation developed for the available, full subsurface data set of clastic rocks (ame: 11 per cent). For bulk TC prediction of clastic rocks, hydrogen index and volume fraction of shale show the largest potential as predictor variable. Bulk density and sonic-log data are questionable input parameters and even the implementation of the photoelectric factor log provides no advantage for reducing the errors. We recommend the use of formation-specific bulk TC equations as developed in this paper for TC prediction in formations that are similar to those

Downloaded from http://gji.oxfordjournals.org/ at Bibliothek des Wissenschaftsparks on November 20, 2013

Table 7. Selected previously published TC prediction equations.

Author	TC prediction equation[a]	Lithotpye eq.[b]	R^2	n	rms [W (m K)$^{-1}$]	ame (per cent)	*SD* [W (m K)$^{-1}$]	Comment	eq.
Tikhomirov (1968)[c]	$\lambda_b = (1.3\exp(0.58\rho_b + 0.4\,WAT))/2.388$	SS, CS, LS	0.61	139	*n.a.*	*n.a.*	*n.a.*	Dry/partially saturated rocks from different authors	(16)
Goss *et al.* (1975)[c]	$\lambda_b = 1.34 - 2.55\phi_N + 0.38V_p$	SiS, GW, SS (cemented)	0.93	39	*n.a.*	10	0.29	TC range: 1.46–3.35, 24 °C, 20 MPa uniax., data from	(17)
Goss & Combs (1976)[c]	$\lambda_b = 0.842 - 3.978\phi_N + 0.695V_p$	SiS, GW, SS (cemented)	0.93	25/14	*n.a.*	10	0.29	Imperial Valley of Southern California	(18)
	$\lambda_b = -4.9\phi_N - 0.160V_p + 3.6\rho_b - 5.5$	SS,SiS, SH, LI, MA, DO, AN	0.81	39(191)	*n.a.*	5–10	*n.a.*	TC range: 1.2–4.2, 29 °C, 7 MPa uniax., cutting samples, Mesozoic sediments, North Sea Basin	(19)
Evans (1977)	$\lambda_b = -0.845 - 2.91(1/V_p) + 1.8\rho_b + 1.714(1/\phi_N)^2 - 3.23\,V_{sh}$	SS	0.30	25	*n.a.*	14.7	0.38		(20)
	$\lambda_b = 1.955 - 0.3(1/V_p) - 0.37\rho_b + 3.139(1/\phi_N)^2 - 1.369\,V_{sh}$	SH, M	0.30	6	*n.a.*	12.1	0.27	TC range: 1–3, core samples, Eocene and Cretaceous	(21)
Vacquier *et al.* (1988)[c]	$\lambda_b = -3.43 + 3.67(1/V_p) + 0.72\rho_b + 7.04(1/\phi_N)^2 - 1.218\,V_{sh}$	SS,SSH	0.50	42	*n.a.*	9.7	0.31	(Parisian Basin), Triassic and Jurassic (Aquitaine Basin)	(22)
	$\lambda_b = 9.15 - 5.116(1/V_p) - 2.663\rho_b + 1.915(1/\phi_N)^2 - 0.5\,V_{sh}$	mixtures	0.66	20	*n.a.*	16.2	0.77		(23)
Hartmann *et al.* (2005)	$\lambda_b = 1.07 + 0.239V_p + 0.504\rho_b + 0.042\phi_N$	SSS	n.a.	>100	0.12	n.a.	n.a.	TC range: 2.5–3.7, cutting samples (Molasse Basin)	(24)
	$\lambda_b = -0.22 + 0.243\,V_p + 0.913\,\rho_b + 1.11\,\phi_N$	SS,DO, LI	n.a.	>100	0.17	n.a.	n.a.		(25)

[a]TC was measured under laboratory conditions (20 °C, 0.1 MPa), otherwise, it is noted above.
[b]Lithological abbreviations (e.g. SS, CS, LS) are described in Appendix A. Statistical paprameters are taken from the original literature.
[c]Equations were reformulated to standard units (conversion see Appendix A).

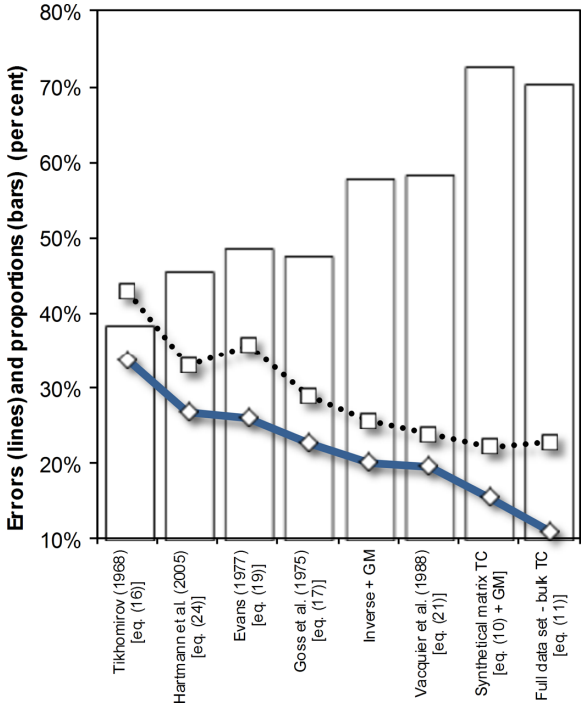

Figure 10. Comparison of results from different prediction methods. Relative ame (blue solid line), relative rms (black dotted line), bars represent proportion of deviations less than 20 per cent.

described in this study. Although afflicted with some error, eq. (11) seems to be a good approximator for clastic rocks in general.

(4) All presented prediction equations show better prediction capabilities than any other previously published approach.

(5) Computed borehole TC profiles may be used as prerequisites for the calculation of temperature profiles with high accuracy (<5 per cent error). This opens up new opportunities, for example (i) to quantify the paleoclimatic effect on a local scale; to estimate the heat-flow density (ii) in the absence of detailed temperature logs and (iii) by using bottom-hole temperature measurements and (iv) to validate temperature maps provided by web-based geothermal information systems.

(6) More work is needed to extend the multimineral rock composition approach to crystalline rocks.

ACKNOWLEDGEMENTS

This work was performed in the framework of the German GeoEn (Verbundvorhaben GeoEnergie-Forschung) project (www.geoen.de). The GeoEn project was funded by the Federal Ministry of Education and Research (BMBF) in the program 'Spitzenforschung und Innovation in den Neuen Ländern'. We are grateful to Ben Norden (GFZ, Potsdam) and the Leibniz Institute for Applied Geophysics (LIAG) in Hannover for providing background data from boreholes, logging data and core material.

REFERENCES

Abdulagatova, Z.Z., Abdulagatov, I.M. & Emirov, S.N., 2009. Effect of temperature and pressure on the thermal conductivity of sandstone, *Int. J. Rock Mech. Min. Sci.,* **46**(6), 1055–1071.

Abdulagatova, Z.Z., Abdulagatov, I.M. & Emirov, S.N., 2010. Effect of pressure, temperature, and oil-saturation on the thermal conductivity of

Downloaded from http://gji.oxfordjournals.org/ at Bibliothek des Wissenschaftsparks Albert Einstein on November 20, 2013

sandstone up to 250 MPa and 520 K, *J. Petrol. Sci. Eng.,* **73**(1–2), 141–155.

Anand, J., Somerton, W. H. & Gomaa, E., 1973. Predicting thermal conductivities of formations from other known properties, *SPE J.,* **13**(5), 267–272.

Asquith, G.B. & Gibson, C.R., 1982. *Basic Well Log Analysis for Geologists,* American Association of Petroleum Geologists.

Balling, N., Kristiansen, J., Breiner, N., Poulsen, K.D., Rasmusen, R. & Saxov, S., 1981. Geothermal measurements and subsurface temperature modelling in Denmark, *Geologiske Skrifter,* **16**(1), 172.

Beck, A.E., 1965. Techniques of measuring heat flow on land, in *Terrestrial Heat Flow,* Vol. **8,** pp. 24–57, ed. Lee, W.H.K., Am. Geophys. Union.

Beziat, A., Dardaine, M. & Mouche, E., 1992. Measurements of the thermal conductivity of clay-sand and clay-graphite mixtures used as engineered barriers for high-level radioactive waste disposal, *Appl Clay Sci,* **6**(4), 245–263.

Birch, F., 1960. The velocity of compressional waves in rocks to 10 kilobars, part 1, *J. geophys. Res.,* **65**(4), 1083–1102.

Birch, F., 1961. The velocity of compressional waves in rocks to 10 kilobars, part 2, *J. geophys. Res.,* **66**(7), 2199–2224.

Blackwell, D.D. & Steele, J.L., 1989. Thermal conductivity of sedimentary rocks; measurement and significance, in *Thermal History of Sedimentary Basins; Methods and Case Histories,* Vol. **14,** pp. 13–36, eds Naeser, N.D. & McCulloh, T.H., Springer.

Brigaud, F. & Vasseur, G., 1989. Mineralogy, porosity and fluid control on thermal conductivity of sedimentary rocks, *Int. J. Rock Mech. Min. Sci.,* **27**(2), A77.

Brigaud, F., Chapman, D.S. & Le Douaran, S., 1990. Estimating thermal conductivity in sedimentary basins using lithologic data and geophysical well logs, *AAPG Bull.,* **74**(9), 1459–1477.

Bullard, E.C. & Day, A., 1961. The fow of heat through the floor of the Atlantic Ocean, *Geophys. J. R. astr. Soc.,* **4**(S1), 282–292.

Buntebarth, G., 1991. Thermal properties of KTB Oberpfalz VB core samples at elevated temperature and pressure, *Sci. Drill.,* **2**(2–3), 73–80.

Čermák, V., 1967. Coefficient of thermal conductivity of some sediments and its dependence on density and water content of rocks, *Chem. Erde-Geochem.,* **26,** 271–278.

Čermák, V. & Rybach, L., 1982. Thermal conductivity and specific heat of minerals and rocks, in *Geophysics—Physical Properties of Rocks,* Vol. **1,** pp. 305–343, eds. Beblo, M. *et al.*, Springer.

Crain, E.R., 2013. Welcome to Crain's Petrophysical Handbook, Online Shareware Petrophysics Training and Reference Manual, urlhttp://www.spec2000.net, Accessed: 2013 April 15.

Dachnov, V.N. & Djakonov, D.J., 1952. *Thermal Investigation of Fissures (in Russian, Термические исследования скважин),* Gostoptehizdat (Гостоптехиздат), Leningrad (Ленинград).

Della Vedova, B. & Von Herzen, R.F., 1987. *Geothermal Heat Flux at the COST B-2 and B-3 Wells, U. S. Atlantic Continental Margin,* Woods Hole Oceanographic Institution.

Demongodin, L., Pinoteau, B., Vasseur, G. & Gable, R., 1991. Thermal conductivity and well logs: a case study in the Paris Basin, *Geophys J. Int.,* **105**(3), 675–691.

Dewan, J.T., 1983. *Essentials of Modern Open-Hole Log Interpretation,* PennWell Books.

Dove, R.E. & Williams, C.F., 1989. Thermal conductivity estimated from elemental concentration logs, *Nucl. Geophys.,* **3**(2), 107–112.

Doveton, J.H., 1986. *Log Analysis of Subsurface Geology: Concepts and Computer Methods,* Wiley-Interscience.

Doveton, J.H. & Cable, H.W., 1979. Fast matrix methods for the lithological interpretation of geophysical logs, *Comput. Geol.,* **3**(–), 101–116.

Doveton, J.H., Förster, A. & Merriam, D.F., 1997. Predicting thermal conductivity from petrophysical logs: a Midcontinent Paleozoic case study, in *Proceedings of the International Association for Mathematical Geology Annual Meeting,* Barcelona, pp. 212–217.

Evans, T.R., 1977. Thermal properties of North Sea rocks, *Log Analyst,* **18**(2), 3–12.

Feldrappe, H., Obst, K. & Wolfgramm, M., 2008. Die mesozoischen Sandsteinaquifere des Norddeutschen Beckens und ihr Potential für die geothermische Nutzung, *Z. geol. Wiss.,* **36**(4–5), 199–222.

Fertl, W.H. & Frost, E. Jr., 1980. Evaluation of shaly clastic reservoir rocks, *J. Petrol. Tech.,* **32**(9), 1641–1646.

Förster, A. *et al.*, 2006. Baseline characterization of the CO2SINK geological storage site at Ketzin, Germany. *Environ. Geosci.,* **13**(3), 145–161.

Förster, A. *et al.*, 2010. Reservoir characterization of a CO_2 storage aquifer: the Upper Triassic Stuttgart formation in the Northeast German Basin, *Mar. Petrol. Geol.,* **27**(10), 2156–2172.

Fuchs, S. & Förster, A., 2010. Rock thermal conductivity of Mesozoic geothermal aquifers in the Northeast German Basin, *Chem. Erde-Geochem.,* **70**(S3), 13–22.

Fuchs, S., Schütz, F., Förster, H.-J. & Förster, A., 2013. Evaluation of common mixing models for calculating bulk thermal conductivity of sedimentary rocks: correction charts and new conversion equations, *Geothermics,* **47,** 40–52.

Gegenhuber, N. & Schön, J., 2012. New approaches for the relationship between compressional wave velocity and thermal conductivity, *J. appl Geophys.,* **76,** 50–55.

Goss, R.D. & Combs, J., 1976. Thermal conductivity measurement and prediction from geophysical well log parameters with borehole application, Final Report, Institute for Geosciences, University of Texas at Dallas, NSF/RA–760364, 31 pp.

Goss, R.D., Combs, J. & Timur, A., 1975. Prediction of thermal conductivity in rocks from other physical parameters and from standard geophysical well logs, in *Proceedings of the SPWLA 16th Annual Logging Symposium, 1975,* 21 pp.

Goutorbe, B., Lucazeau, F. & Bonneville, A., 2006. Using neural networks to predict thermal conductivity from geophysical well logs, *Geophys. J. Int.,* **166**(1), 115–125.

Griffiths, C.M., Brereton, N.R., Beausillon, R. & Castillo, D., 1992. Thermal conductivity prediction from petrophysical data: a casestudy, *Spec. Publ. Geol. Soc. Lond.,* **65**(1), 299–315.

Gröber, H., Erk, S. & Grigull, U., 1955. *Die Grundgesetze der Wärmeübertragung,* Springer.

Hartmann, A., Rath, V. & Clauser, C., 2005. Thermal conductivity from core and well log data, *Int. J. Rock Mech. Min. Sci.,* **42**(7–8), 1042–1055.

Hartmann, A., Pechnig, R. & Clauser, C., 2008. Petrophysical analysis of regional-scale thermal properties for improved simulations of geothermal installations and basin-scale heat and fluid flow, *Int. J. Earth Sci.,* **97**(2), 421–433.

Hesshaus, A., Heinig, S., Kringel, R. & Röhling, H.-G., 2010. GeneSys Hannover—hydrochemische und petrographische Untersuchungen an der Geothermiebohrung Groß Buchholz GT1, in *Proceedings of the Geothermiekongress 2010,* 17–19. November 2010, Karlsruhe, 10 pp.

Horai, K.-I., 1971. Thermal conductivity of rock-forming minerals, *Geophys. Res. Lett.,* **76**(5), 1278–1308.

Horai, K.-I. & Simmons, G., 1969. Thermal conductivity of rock-forming minerals, *Earth planet. Sci. Lett.,* **6**(5), 359–368.

Houbolt, J.J.H.C. & Wells, P.R.A., 1980. Estimation of heat flow in oil wells based on a relation between heat conductivity and sound velocity, *Geol. Mijnbouw-N. J. G.,* **59**(3), 215–224.

Hübner, W., Hunze, S., Baumgarten, H., Orilski, J. & Wonik, T., 2012. Petrophysical and sedimentary petrographic characterisation of the Bückeburg Formation (German Wealden) in the geothermal well Groß Buchholz Gt-1 (Hanover, Germany), *Z. Deut. Gesell. Geowissenschaften,* **163**(4), 483–492.

Hurtig, E. & Brugger, H., 1970. Wärmeleitfähigkeitsmessung unter einaxialem Druck, *Tectonophysics,* **10**(1–3), 67–77.

Karl, R., 1965. Gesteinsphysikalische Parameter (Schallgeschwindigkeit und Wärmeleitfähigkeit), *Freiberger Forschungshefte,* **C197,** 7–76.

Khandelwal, M., 2010. Prediction of thermal conductivity of rocks by soft computing, *Int. J. Earth Sci.,* **100**(6), 1–7.

Kukkonen, I.T. & Peltoniemi, S., 1998. Relationships between thermal and other petrophysical properties of rocks in Finland, *Phys. Chem. Earth.,* **23**(3), 341–349.

Downloaded from http://gji.oxfordjournals.org/ at Bibliothek des Wissenschaftsparks on November 20, 2013

Lemmon, E.W., McLinden, M.O. & Friend, D.G., 2005. *Thermophysical Properties of fluid systems, NIST Chemistry WebBook,* NIST Standard Reference Database, 20 899 pp.

Lichtenecker, K., 1924. Der elektrische Leitungswiderstand künstlicher und natürlicher Aggregate, *Physik Zeitschr,* **25**(8), 169–181, 193–204, 226–233.

Lovell, M.A., 1985. Thermal conductivity and permeability assessment by electrical resistivity measurements in marine sediments, *Mar. Geotechnol.,* **6**(2), 205–240.

Lovell, M.A. & Ogden, P., 1984. *Remote Assessment of Permeability/thermal Diffusivity of Consolidated Clay Sediments: Final Report,* Nuclear Science and Technology, Commission of the European Communities, Directorate-General Science, Research and Development, 123 pp.

Merkel, R.H., Maccary, L.M. & Chico, R.S., 1976. Computer techniques applied to formation evaluation, *Log Analyst,* **17**(3), 3–10.

Midttømme, K., Roaldset, E. & Aagaard, P., 1997. Thermal conductivity of argillaceous sediments, in *Modern Geophysics in Engineering Geology,* Vol. **12,** pp. 355–363, eds. McCann, D.M., Eddleston, M., Fenning, P.J. & Reeves, G.M., Geological Society Engineering Geology.

Moiseyenko, U.I., Sokolova, L.S. & Istomin, V.E., 1970. *Electrical and Thermal Properties of Rocks (in Russian: Elektricheskiye i teplovyye svoystva gornykh porod v usloviyakh normalnykh i vysokikh temperatur i davleniy),* Epaminond Ėpaminondovič Fotiadi, Novosibirsk, Russia.

Molnar, P.S. & Hodge, D., 1982. Correlation of thermal conductivity with physical properties obtained from geophysical well logs, in *Proceedings of the AAPG Annual Convention with Divisions SEPM/EMD/DPA,* June 27–30, 1982, Calgary, AB, Canada, 608–609 pp.

Norden, B., Förster, A., Vu-Hoang, D., Marcelis, F., Springer, N. & Le Nir, I., 2010. Lithological and petrophysical core-log interpretation in CO2SINK, the European CO_2 onshore research storage and verification project, *SPE Res. Eval. Eng.,* **13**(2), 179–192.

Orilski, J., Schellschmidt, R. & Wonik, T., 2010. Temperaturverlauf und Wärmeleitfähigkeit im Untergrund der Bohrung Groß Buchholz GT1 in Hannover, in *Proceedings of the Geothermiekongress 2010,* 17–19 November 2010, Karlsruhe, 10 pp.

Özkahraman, H.T., Selver, R. & Işık, E.C., 2004. Determination of the thermal conductivity of rock from P-wave velocity, *Int. J. Rock Mech. Min. Sci.,* **41**(4), 703–708.

Popov, Y., Tertychnyi, V., Romushkevich, R., Korobkov, D. & Pohl, J., 2003. Interrelations between thermal conductivity and other physical properties of rocks: experimental data, *Pure appl. Geophys.,* **160**(5–6), 1137–1161.

Popov, Y., Romushkevich, R., Korobkov, D., Mayr, S., Bayuk, I., Burkhardt, H. & Wilhelm, H., 2011. Thermal properties of rocks of the borehole Yaxcopoil-1 (Impact Crater Chicxulub, Mexico), *Geophys. J. Int.,* **184**(2), 729–745.

Popov, Y.A., Pribnow, D.F.C., Sass, J.H., Williams, C.F. & Burkhardt, H., 1999. Characterization of rock thermal conductivity by high-resolution optical scanning, *Geothermics,* **28**(2), 253–276.

Poulsen, K.D., Saxov, S., Balling, N. & Kristiansen, J.I., 1981. Thermal conductivity measurements on Silurian limestones from the Island of Gotland, Sweden, *Geologiska Foreningen i Stockholm Forhandlingar,* **103**(3), 349–356.

Pribnow, D., Williams, C.F. & Burkhardt, H., 1993. Well log-derived estimates of thermal conductivity in crystalline rocks penetrated by the 4-KM deep KTB Vorbohrung, *Geophys. Res. Lett.,* **20**(12), 1155–1158.

Quirein, J., Kimminau, S., La Vigne, J., Singer, J. & Wendel, F., 1986. A coherent framework for developing and applying multiple formation evaluation models, in *Proceedings of the SPWLA 27th Annual Logging Symposium*, Houston. June 9–13, 17 pp.

Röhling, H.-G. & Heinig, S., 2012. Lithostratigraphie und Petrographie des Mittleren Buntsandsteins in der Geothermiebohrung Groß Buchholz Gt1 und der Bohrung Hämelerwald Z1, *Erdöl Erdgas Kohle,* **128**(4), 144–153.

Sahlin, T. & Middleton, M.F., 1997. Correlation of thermal conductivity with well log derived petrophysical parameters, in *Proceedings of the Second Nordic Symposium on Petrophysics,* Reykjavík, Orkustofnun, 263–281 pp.

Sass, J.H., Lachenbruch, A.H. & Munroe, R.J., 1971. Thermal conductivity of rocks from measurements on fragments and its application to heat-flow determinations, *J. geophys. Res.,* **76**(14), 3391–3401.

Savre, W.C., 1963. Determination of a more accurate porosity and mineral composition in complex lithologies with the use of the sonic, neutron and density Surveys, *J. Petrol. Tech.,* **15**(9), 945–959.

Schäfer, F. *et al.*, 2012. Kurzprofil der Geothermiebohrung Groß Buchholz Gt 1, *Erdöl Erdgas Kohle,* **128**(1), 20–26.

Schön, J., 1983. *Petrophysik. Physikalische Eigenschaften von Gesteinen und Mineralien,* Enke Ferdinand.

Schön, J.-H., 1996. Physical properties of rocks, fundamentals and principles of petrophysics, in *Handbook of Geophysical Exploration: Seismic Exploration,* Vol. **18,** pp. 583, eds Helbig, K. & Treitel, S., Pergamon.

Seipold, U. & Huenges, E., 1998. Thermal properties of gneisses and amphibolites—high pressure and high temperature investigations of KTB-rock samples, *Tectonophysics,* **291**(1–4), 173–178.

Serra, O., 1984. *Fundamentals of Well-Log Interpretation—The Acquisition of Logging Data,* Elsevier.

Simmons, G., 1964a. Velocity of compressional waves in various minerals at pressures to 10 kilobars, *J. geophys. Res.,* **69**(6), 1117–1121.

Simmons, G., 1964b. Velocity of shear waves in rocks to 10 kilobars, 1, *J. geophys. Res.,* **69**(6), 1123–1130.

Singh, R., Bhoopal, R.S. & Kumar, S., 2011. Prediction of effective thermal conductivity of moist porous materials using artificial neural network approach, *Build Environ.,* **46**(12), 2603–2608.

Singh, T.N., Sinha, S. & Singh, V.K., 2007. Prediction of thermal conductivity of rock through physico-mechanical properties, *Build Environ.,* **42**(1), 146–155.

Somerton, W.H., 1992. *Thermal Properties and Temperature-Related Behavior of Rock/Fluid Systems,* Elsevier Science Publishers B.V.

Sundberg, A., 2002. Determination of thermal properties at Äspö HRL. Comparison and evaluation of methods and methodologies for borehole KA 2599 G01, SKB Rapport, SKB, pp.

Sundberg, J., Back, P.-E., Ericsson, L.O. & Wrafter, J., 2009. Estimation of thermal conductivity and its spatial variability in igneous rocks from in situ density logging, *Int. J. Rock Mech. Min. Sci.,* **46**(6), 1023–1028.

Thornton, W.M., 1924. CI. The thermal conductivity of solid electric insulators—II, *Phil. Mag. Ser. 6,* **48**(288), 1054–1056.

Tikhomirov, V.M., 1968. The thermal conductivity of rocks and its relationship to density, moisture content, and temperature (in Russian), *Neftânoe Hozâjstvo,* **46**(4), 36–40.

Vacquier, V., 1985. The measurement of thermal conductivity of solids with a transient linear heat source on the plane surface of a poorly conducting body, *Earth planet. Sci. Lett.,* **74**(2–3), 275–279.

Vacquier, V., Mathieu, Y., Legendre, E. & Blondin, E., 1988. Experiment on estimating thermal conductivity of sedimentary rocks from oil well logging, *Int. J. Rock Mech. Min. Sci.,* **26**(2), 63–63.

Vasseur, G., Brigaud, F. & Demongodin, L., 1995. Thermal conductivity estimation in sedimentary basins, *Tectonophysics,* **244**(1–3), 167–174.

Von Herzen, R. & Maxwell, A.E., 1959. The measurement of thermal conductivity of deep-sea sediments by a needle-probe method, *J. geophys. Res.,* **64**(10), 1557–1563.

Walsh, J.B. & Decker, E.R., 1966. Effect of pressure and saturating fluid on the thermal conductivity of compact rock, *J. geophys. Res.,* **71**(12), 3053–3061.

Western Atlas International, 1995. *Introduction to Wireline Log Analysis,* Houston, 312 pp.

Whitney, D.L. & Evans, B.W., 2010. Abbreviations for names of rock-forming minerals, *Am. Miner.,* **95**(1), 185–187.

Williams, C.F. & Anderson, R.N., 1990. Thermophysical properties of the Earth's crust: in situ measurements from continental and ocean drilling, *J. geophys. Res.,* **95**(6), 9209–9236.

Woodside, W. & Messmer, J.H., 1961. Thermal conductivity of porous media. II. Consolidated rocks, *J. appl. Geophys.,* **32**(9), 1699–1706.

Wyllie, M.R.J., Gregory, A.R. & Gardner, G.H.F., 1958. An experimental investigation of factors affecting elastic wave velocities in porous media, *Geophysics,* **23**(3), 459–493.

Downloaded from http://gji.oxfordjournals.org/ at Bibliothek des Wissenschaftsparks Albert Einstein on November 20, 2013

Zamora, M., Dung, V.T., Bienfait, G. & Poirier, J.P., 1993. An empirical relationship between thermal conductivity and elastic wave velocities in sandstone, *Geophys. Res. Lett.,* **20**(16), 1679–1682.
Zierfuss, H. & van der Vliet, G., 1956. Laboratory measurements of heat conductivity of sedimentary rocks, *AAPG Bull.,* **40**(10), 2475–2488.

APPENDIX A: NOMENCLATURE

Subscripts:

b	bulk
fl	fluid
i	index of point
lab	laboratory
ma	matrix
maa	apparent matrix
max	maximum
mea	measured
min	minimum
ND	neutron–density
p	pore
sh	shale
z	depth level

Litho:

AS	anhydrite
CS	claystone
DO	dolomite
GW	greywacke
LI	limestone
M	mudstone
MA	marlstone
sh	shale
SiS	siltstone
SS	sandstone
SSH	sandy shale
SSS	shaly sandstone

Statistics:

am	arithmetic mean
ame	arithmetic mean error
B_{si}	standardized beta coefficients for input variable i
cv	coefficient of variation
df.	degree of freedom
F	*F*-value
n	number of samples
p	significance level
rms	root mean square error
R^2	coefficient of determination
SD	standard deviation
T	tolerance

Well logging:

ANN	artificial neural networks
ΔT	sonic interval transit time (DT) [μs m^{-1}]
γ	(natural) gamma ray (GR) [API]
gradT	temperature gradient [K km^{-1}]
MLR	multiple linear regression
NLR	non-linear regression
ϕ_D	density porosity [p.u.]
ϕ_e	effective porosity (Phie) [p.u.]
ϕ_N	neutron porosity (hydrogen index, PHIN) [p.u.]
ϕ_S	sonic porosity [p.u.]
ϕ_t	total porosity [p.u.]
p	pressure [MPa]
P_e	photoelectric factor log [pe]
q	heat-flow density [mW m^{-2}]
ρ_b	bulk density (RHO$_b$) [g cm^{-3}]
ρ_m	matrix density (RHO$_{ma}$) [g cm^{-3}]
SLR	simple linear regression
TC	thermal conductivity [W (m K)$^{-1}$]
T	temperature [°C; K]
U	photoelectric absorption index [barns cm^{-3}]
VP	sonic velocity [km s^{-1}]
V_{sh}	volume fraction of shale [–]
WAT	water content [–]

Conversion:

Thermal conductivity: 1 W (m K)$^{-1}$ = 2.388 mcal (cm s K)$^{-1}$ = 0.578 Btu (hr ft F)$^{-1}$
Sonic interval transit time: 1 μs ft^{-1} = 304.799 km s^{-1}

APPENDIX B: MATRIX-TC EQUATIONS FOR VARIABLE WELL-LOG COMBINATIONS

Downloaded from http://gji.oxfordjournals.org/ at Bibliothek des Wissenschaftsparks on November 20, 2013

Eq.	No. of logs	Matrix-thermal-conductivity-prediction equations [MTC in W (mK)$^{-1}$] Unstandardized regression coefficients Constant	Predictor variables/Log combinations					Artificial data set Regression set				Validation Artificial data set Testing set			Subsurface data set All samples		
		b_0 [–]	RHO_{ma} [g cm^{-3}]	$PHIN_{ma}$ [–]	U_{ma} [barns cm^{-3}]	DT_{ma} [μs m^{-1}]	V_{sh} [–]	R^2 [–]	F	T^1	p	ame [per cent]	SD [per cent]	rms [per cent]	ame [per cent]	SD [per cent]	rms [per cent]
Evaporites								$n = 41$				$n = 10$					
–		–	VSH ist not correlated to the set of evaporite rocks														
A1	1	13.418	–3.488					0.251	14.4	1.00	<0.001	51.4 per cent	72.3 per cent	85.7 per cent			
A2	1	5.527		–10.483				0.665	80.47	1.00	<0.001	19.2 per cent	12.7 per cent	22.7 per cent			
A3	1	–0.213			0.414			0.145	7.785	1.00	0.008	45.4 per cent	44.6 per cent	62.0 per cent			
A4	1	–3.200				0.043		0.533	46.73	1.00	<0.001	37.7 per cent	55.1 per cent	64.5 per cent			
Eq. 7	2	14.060	–3.375	–10.350				0.922	237.4	1.00	<0.001	7.0 per cent	5.6 per cent	8.8 per cent			
A5	2	8.584	–3.346		0.386			0.383	13.41	1.00	<0.001	40.4 per cent	58.5 per cent	68.7 per cent			
A6	2	–24.667	5.434			0.086		0.647	37.70	0.18	<0.001	30.5 per cent	32.3 per cent	43.2 per cent			
A7	2	5.477		–10.458	0.004			0.656	39.21	0.76	<0.001	19.2 per cent	12.8 per cent	22.7 per cent	no data available		
A8	2	–0.193		–8.262		0.031		0.913	210.7	0.89	<0.001	10.0 per cent	7.4 per cent	12.2 per cent			
A9	2	–4.849			0.198	0.040		0.557	26.18	0.90	<0.001	34.2 per cent	51.5 per cent	59.6 per cent			
A10	3	14.403	–3.383	–10.515	–0.027			0.920	155.3	0.41	<0.001	7.0 per cent	5.4 per cent	8.6 per cent			
A11	3	9.438	–2.310	–9.642		0.010		0.923	160.3	0.09	<0.001	7.6 per cent	6.0 per cent	9.5 per cent			
A12	3	–25.030	5.557		–0.015	0.087		0.638	24.48	0.11	<0.001	30.1 per cent	31.2 per cent	42.3 per cent			
A13	3	0.893		–8.840	–0.105	0.032		0.919	152.4	0.73	<0.001	8.4 per cent	6.5 per cent	10.4 per cent			
A14	4	8.108	–1.831	–9.713	–0.065	0.015		0.923	121.5	0.08	<0.001	7.3 per cent	5.5 per cent	9.0 per cent			
Carbonates									$n = 2,252$				$n = 562$				
A15	1	–5.983	3.598					0.285	897.2	1.00	<0.001	15.3 per cent	13.7 per cent	20.5 per cent			
A16	1	4.195		–7.439				0.349	1208	1.00	<0.001	15.1 per cent	11.4 per cent	18.9 per cent			
A17	1	3.599			–0.032			0.004	9.265	1.00	0.002	19.0 per cent	15.4 per cent	24.4 per cent			
A18	1	10.537				–0.039		0.480	2076	1.00	<0.001	12.4 per cent	8.5 per cent	15.0 per cent			
A19	1	4.785					–2.882	0.702	5306	1.00	<0.001	9.2 per cent	6.8 per cent	11.5 per cent			
A20	2	–2.139	2.366	–5.634				0.451	927.3	0.83	<0.001	13.8 per cent	10.3 per cent	17.2 per cent			
A21	2	–11.369	6.847		–0.365			0.589	1614	0.57	<0.001	12.8 per cent	10.9 per cent	16.8 per cent			
A22	2	7.968	0.702			–0.035		0.485	1061	0.52	<0.001	12.3 per cent	8.5 per cent	15.0 per cent			
Eq. 9	2	5.058	–0.099				–2.915	0.702	2654	0.58	<0.001	9.2 per cent	6.8 per cent	11.5 per cent			
A23	2	5.324		–8.314	–0.124			0.406	769.7	0.92	<0.001	14.5 per cent	12.4 per cent	19.1 per cent			
A24	2	9.472		–2.135		–0.032		0.492	1092	0.45	<0.001	12.3 per cent	8.5 per cent	14.9 per cent			
A25	2	4.782		4.550			–3.921	0.741	3229	0.30	<0.001	8.3 per cent	6.7 per cent	10.6 per cent			
A26	2	15.673			–0.274	–0.055		0.706	2701	0.75	<0.001	9.9 per cent	7.6 per cent	12.5 per cent			
A27	2	6.913			–0.222		–3.461	0.872	7639	0.86	<0.001	6.9 per cent	5.6 per cent	8.9 per cent			
A28	2	–0.683				0.035	–4.870	0.755	3474	0.14	<0.001	8.7 per cent	6.4 per cent	10.8 per cent			
A29	3	–7.507	5.627	–5.753	–0.370			0.763	2417	0.51	<0.001	10.1 per cent	7.3 per cent	12.4 per cent	no data available		
A30	3	5.656	0.984	–2.572		–0.025		0.503	759	0.27	<0.001	12.2 per cent	8.4 per cent	14.8 per cent			
A31	3	6.780	–0.725	5.143			–4.296	0.747	2221	0.19	<0.001	8.0 per cent	6.7 per cent	10.4 per cent			
A32	3	3.733	3.875		–0.393	–0.039		0.835	3804	0.39	<0.001	7.4 per cent	5.4 per cent	9.2 per cent			
Eq. 8	3	–0.550	3.093		–0.332		–2.727	0.952	14892	0.38	<0.001	4.2 per cent	3.2 per cent	5.3 per cent			
A33	3	–2.947	0.625			0.039	–4.860	0.760	2372	0.12	<0.001	9.2 per cent	6.9 per cent	11.5 per cent			
A34	3	15.255		–0.707	–0.270	–0.052		0.707	1812	0.35	<0.001	9.9 per cent	8.2 per cent	12.9 per cent			
A35	3	6.995		5.253	–0.231		–4.683	0.924	9110	0.28	<0.001	5.3 per cent	4.6 per cent	7.0 per cent			
A36	3	–1.591		5.523		0.041	–6.459	0.812	3239	0.09	<0.001	7.5 per cent	6.1 per cent	9.7 per cent			
A37	3	5.288			–0.207	0.010	–3.961	0.875	5238	0.11	<0.001	7.2 per cent	5.9 per cent	9.2 per cent			
A38	4	2.084	4.049	–1.882	–0.389	–0.031		0.845	3060	0.26	<0.001	7.9 per cent	5.9 per cent	9.9 per cent			
A39	4	0.838	2.540	3.444	–0.318		–3.660	0.972	19500	0.18	<0.001	3.1 per cent	2.9 per cent	4.2 per cent			
A40	4	–1.573	–0.005	5.526		0.041	–6.460	0.812	2428	0.09	<0.001	7.5 per cent	6.1 per cent	9.7 per cent			
A41	4	–3.145	3.176		–0.313	0.014	–3.445	0.959	13111	0.11	<0.001	4.0 per cent	3.0 per cent	5.0 per cent			
A42	4	4.389		5.546	–0.207	0.015	–5.556	0.932	7700	0.09	<0.001	4.9 per cent	4.7 per cent	6.8 per cent			
A43	5	–2.206	2.594	3.732	–0.294	0.017	–4.613	0.982	24473	0.08	<0.001	2.4 per cent	2.8 per cent	3.7 per cent			

Downloaded from http://gji.oxfordjournals.org/ at Bibliothek des Wissenschaftsparks Albert Einstein on November 20, 2013

Eq.	No. of logs	Matrix-thermal-conductivity-prediction equations [MTC in W (mK)$^{-1}$] Unstandardized regression coefficients Predictor variables/Log combinations Constant						Artificial data set Regression set				Artificial data set Testing set			Validation Subsurface data set All samples		
		b_0 [–]	RHO_{ma} [g cm^{-3}]	$PHIN_{ma}$ [–]	U_{ma} [barns cm^{-3}]	DT_{ma} [μs m^{-1}]	V_{sh} [–]	R^2 [–]	F	T^1	p	ame [per cent]	*SD* [per cent]	rms [per cent]	ame [per cent]	*SD* [per cent]	rms [per cent]
Clastics								*n = 21,617*				*n = 5,404*					
A44	1	−3.684	2.534					0.110	2676	1.00	<0.001	20.8 per cent	15.3 per cent	25.8 per cent	19.5 per cent	13.6 per cent	29.9 per cent
A45	1	4.171		−16.473				0.585	30498	1.00	<0.001	14.1 per cent	11.0 per cent	17.9 per cent	25.2 per cent	65.9 per cent	79.6 per cent
A46	1	4.126			−0.144			0.072	1667	1.00	<0.001	21.4 per cent	15.3 per cent	26.3 per cent	21.1 per cent	12.9 per cent	40.2 per cent
A47	1	12.532				−0.051		0.312	9819	1.00	<0.001	17.9 per cent	13.1 per cent	22.2 per cent	45.0 per cent	77.3 per cent	88.7 per cent
A48	1	4.783					−3.382	0.688	47759	1.00	<0.001	11.8 per cent	9.3 per cent	15.0 per cent	15.4 per cent	11.1 per cent	35.0 per cent
A49	2	−2.889	2.703	−16.692				0.711	26531	1.00	<0.001	11.5 per cent	8.8 per cent	14.5 per cent	26.5 per cent	85.3 per cent	97.4 per cent
A50	2	−10.721	6.613		−0.444			0.509	11199	0.58	<0.001	15.4 per cent	12.3 per cent	19.7 per cent	26.8 per cent	38.3 per cent	108.5 per cent
A51	2	8.691	1.115			−0.046		0.331	5343	0.87	<0.001	17.8 per cent	13.2 per cent	22.2 per cent	41.7 per cent	75.0 per cent	84.9 per cent
A52	2	3.385	0.515				−3.292	0.692	24337	0.89	<0.001	11.7 per cent	9.2 per cent	14.9 per cent	15.4 per cent	12.0 per cent	36.2 per cent
A53	2	3.371		−19.199	0.122			0.621	17715	0.69	<0.001	13.2 per cent	10.0 per cent	16.5 per cent	27.4 per cent	81.0 per cent	88.6 per cent
A54	2	8.031		−13.938		−0.022		0.627	18174	0.75	<0.001	13.0 per cent	10.0 per cent	16.4 per cent	33.0 per cent	97.1 per cent	97.6 per cent
Eq. 10	2	5.281		−2.961			−2.797	0.430	1336	0.55	<0.001	11.4 per cent	9.1 per cent	14.7 per cent	15.7 per cent	15.8 per cent	22.3 per cent
A55	2	12.995			−0.108	−0.049		0.352	5884	0.99	<0.001	17.1 per cent	12.9 per cent	21.4 per cent	44.5 per cent	72.9 per cent	83.9 per cent
A56	2	4.901			−0.017		−3.346	0.689	23980	0.92	<0.001	11.8 per cent	9.3 per cent	15.0 per cent	15.5 per cent	11.1 per cent	36.9 per cent
A57	2	0.308				0.027	−4.331	0.719	27641	0.36	<0.001	11.5 per cent	9.5 per cent	14.9 per cent	17.9 per cent	19.5 per cent	89.8 per cent
A58	3	−4.913	3.779	−14.106	−0.120			0.725	19016	0.29	<0.001	11.2 per cent	8.8 per cent	14.3 per cent	24.9 per cent	78.7 per cent	100.4 per cent
A59	3	−1.224	2.501	−15.930		−0.006		0.713	17940	0.61	<0.001	11.7 per cent	9.2 per cent	14.9 per cent	28.4 per cent	92.4 per cent	98.0 per cent
A60	3	−0.092	1.748	−10.097			−1.449	0.730	19441	0.15	<0.001	10.8 per cent	8.6 per cent	13.8 per cent	19.0 per cent	50.2 per cent	65.9 per cent
A61	3	6.770		−16.538	0.099	−0.018		0.649	13340	0.50	<0.001	12.5 per cent	9.9 per cent	15.9 per cent	31.5 per cent	105.3 per cent	105.4 per cent
A62	3	4.454		−6.175	0.035		−2.464	0.703	17076	0.17	<0.001	11.3 per cent	9.0 per cent	14.4 per cent	17.2 per cent	26.9 per cent	43.3 per cent
A63	3	0.528		−0.630		0.025	−4.181	0.719	18441	0.09	<0.001	11.0 per cent	8.6 per cent	13.9 per cent	16.8 per cent	18.2 per cent	83.7 per cent
A64	3	0.287			0.001	0.027	−4.337	0.719	18427	0.32	<0.001	11.4 per cent	9.3 per cent	14.7 per cent	17.9 per cent	19.4 per cent	89.4 per cent
A65	3	−2.358	0.807			0.029	−4.292	0.729	19335	0.35	<0.001	10.9 per cent	8.4 per cent	13.7 per cent	18.5 per cent	20.3 per cent	93.4 per cent
A66	3	−4.294	5.348		−0.372	−0.020		0.539	8418	0.38	<0.001	14.6 per cent	11.3 per cent	18.5 per cent	32.2 per cent	55.0 per cent	75.3 per cent
A67	3	−0.096	2.159		−0.139		−2.700	0.713	17897	0.30	<0.001	11.3 per cent	9.1 per cent	14.6 per cent	16.9 per cent	17.9 per cent	58.3 per cent
A68	4	−3.872	3.609	−13.811	−0.114	−0.004		0.726	14325	0.28	<0.001	11.2 per cent	8.5 per cent	14.0 per cent	26.1 per cent	83.0 per cent	97.2 per cent
A69	4	−2.119	2.758	−8.783	−0.099		−1.267	0.739	15328	0.15	<0.001	10.6 per cent	8.6 per cent	13.7 per cent	18.8 per cent	49.8 per cent	74.7 per cent
A70	4	−2.336	1.479	−6.441		0.018	−2.726	0.738	15232	0.06	<0.001	10.7 per cent	8.5 per cent	13.6 per cent	14.3 per cent	17.5 per cent	77.9 per cent
A71	4	−5.336	2.314		−0.129	0.028	−3.703	0.746	15867	0.25	<0.001	10.5 per cent	8.4 per cent	13.4 per cent	20.4 per cent	23.7 per cent	112.9 per cent
A72	4	0.569		−1.194	0.010	0.024	−4.087	0.719	13842	0.07	<0.001	11.1 per cent	8.5 per cent	14.0 per cent	16.6 per cent	18.0 per cent	79.7 per cent
A73	5	−4.917	2.576	−4.466	−0.111	0.020	−2.697	0.750	12986	0.06	<0.001	10.4 per cent	8.2 per cent	13.3 per cent	15.4 per cent	18.3 per cent	96.3 per cent

[1]For equations with more than 3 predictor variables, the lowest tolerance value is noted. For statistics see Section 3.3, for abbreviations see the Appendix A.

Downloaded from http://gji.oxfordjournals.org/ at Bibliothek des Wissenschaftsparks [redacted] on November 20, 2013